Mutations in *atpG* affect postranscriptional expression of *pckA* in *Escherichia coli*

A thesis submitted to the College of Graduate Studies and Research in partial fulfilment of the requirements for the Degree of Masters of sciences
in the Department of Microbiology and Immunology University of Saskatchewan

By

Jasnehta Permala-Booth

Permission to Use

In presenting this thesis in partial fulfillment of the requirements for a Postgraduate degree from the University of Saskatchewan, I agree that the libraries of this University may make it freely available for inspection. I further agree that permission for copying of this thesis in any manner, in whole or in part, for scholarly purposes may be granted by the professor or professors who supervised my thesis work or, in their absence, by the head of the department or the Dean of the college in which my thesis work was done. It is understood that any copying or publication or use of this thesis or parts thereof for financial gain shall not be allowed without my written permission. It is also understood that due recognition shall be given to me and to the University of Saskatchewan in ay scholarly use which may be made of any material in my thesis.

Requests for permission to copy or make other use of material in this thesis in whole or in part should be addresses to:

Head of the Department of Microbiology and immunology
107 Wiggins Road
University of Saskatchewan
Saskatoon, Saskatchewan
Canada S7N5E5

Abstract

Prokaryotic cells such as *Escherichia coli* use glucose as their preferred carbon source. In the absence of glucose, these cells resort to other sources to generate glucose and this process of *de novo* synthesis of glucose is termed gluconeogenesis. Phosphoenolpyruvate carboxykinase (Pck) is one of the three enzymes important in regulating gluconeogenesis. It converts oxaloacetic acid (OAA) from the Krebs cycle to phosphoenolpyruvate (PEP), a glycolytic intermediate. The Pck structural gene (*pckA*) is regulated by catabolite repression. There is a 100-fold induction of *pckA-lacZ* fusions at the onset of stationary phase concurrent with induction of glycogen synthesis. Mutants affecting the expression of *pckA* were analysed to shed some light on the mechanism of its genetic regulation.

Spontaneous mutants isolated with Pck^- (lack of PEP carboxykinase activity) and Suc^- (inability to utilise succinate as carbon source) phenotypes were previously characterised as *atpG* mutants defective in the γ subunit of ATP synthase.

In this work we find by reverse transcriptase and real time quantitative PCR that levels of *pckA* mRNA are normal in the *atpG* mutants and that the defects in expression of *pckA* are therefore likely at the level of translation, protein assembly and/or protein degradation. As expected, ATP synthase activity and proton pumping in inside-out membrane vesicles were defective in these *atpG* mutants. It is likely that one of these defects is affecting regulation or expression of the *pckA* gene. It was observed that *atpG* mutants were defective in calcium-dependent transformation although they could be made competent for electroporation. The *atpG* mutants were also defective for growth of P1 bacteriophage although they could serve as recipients for P1-dependent generalised

transduction. These latter phenotypes are also likely due to defects in energy metabolism.

ACKNOWLEDGEMENTS

Firstly, I would like to express my gratitude to my supervisor, Dr. Goldie, who has been a nurturing mentor during my study. I would also like to thank the members of the committee: Drs. Harold Bull and Peter Howard for their guidance.

I thank Drs. Vikram Misra, Phil Gobeil, Oksana Akhova from Veterinary Microbiology and Dr. Rozwadoski and Tricia Kreiser from Agriculture Canada for allowing me to use their real time (qPCR) cycler and for their support and advice in using the qPCR cycler. I would also like to thank Dr. George Mackie for the revised protocol for RNA extraction. My thank also goes to Jayaum Booth for his technical advice in qPCR. I also want to thank Dr. J Lee and personnel from his lab in the Department of Biochemistry for their help in using the Hitachi F-2500 FL spectrophotometer. I would also like to thank Mary Woodsworth from Microbiology and Immunology for technical support and advice.

My thanks to members of my lab, Seema Madhavan, Deng Mapiour, Babak Rajabi for the numerous discussions, science or otherwise.

I greatly appreciate the financial support provided by the Department of Microbiology and Immunology and by the College of Medicine Graduate Scholarships. This work was supported by grant from the Natural Science and Engineering Research Council of Canada (NSERC).

Lastly, I would like to express my gratitude to my parents, sibblings and husband, whose sacrifice, love, guidance and support made me the person I am today. They have provided me with everything in life to make me successful. My smile will always reflect the love, happiness you instilled in me. Thank you.

To my parents, husband and sibblings

Table of Contents

List of Tables

List of Figures

List of Abbreviations

aceA	isocitrate lyase gene
aceB	malate synthase A gene
ADP	adenosine biphosphate
Amp^R	ampicillin resistant
ANSA	1-amino-2 naphthol-4 sulfonic acid
ATP	adenosine triphosphate
ATPase	ATP synthase
atp	genes of the operon encoding ATPase
Atp	phenotype: normal or low ATPase activity
bp	base pair
BSA	bovine serum albumin
cAMP	cyclic adenosine 3'-5' monophosphate
Cam^R	chloramphenical resistant
CCCP	carbonyl cyanide-3-chlorophenylhydrazone
cDNA	complementary DNA
Crp	Cyclic AMP receptor protein
crr	Catabolite repression resistance: glucose phosphotransferase Enzyme IIA
csrA	carbon storage regulator gene
C_t	comparative threshold
CTAB	cetyl tetra ammonium bromide (hexadecyl tetra ammonium bromide)
cya	adenylate cyclise gene
cydA	cytochrome *d* oxidase subunit I gene
dATP	2'-deoxyadenosine 5' -triphosphate
DCCD	1,3-dicyclohexylcarbodiimide
dCTP	2' -deoxycytidine 5'-triphosphate
dGTP	2'-deoxyguanosine 5'-triphosphate
DNA	deoxyribonucleic acid
DnaK	chaperone protein (heat shock protein family 70 protein)
dsrA	Downstream region: gene for small RNA regulator of RpoS and H-NS
dUTP	2'-deoxyuridine 5'-triphosphate
E. coli K12	*Escherichia coli* strain K12
EDTA	ethylenediminotetraacetic acid
endA1	endonuclease I gene
FAM	6-carboxy-fluorescein
Fbp	fructose-bis-phosphatase
FruR	repressor of fructose operon

g	gravitational force
GFP	green fluorescence protein
glgB	1,4-α-glucan branching enzyme gene
glgC	glucose-1-phosphate adenylyltransferase gene
glnG	nitrogen regulation protein I gene
gltA	citrate synthase gene
Gro	growth yield phenotype
HU	DNA-binding protein II
H-NS	Heat-stable nucleoid-structuring protein
icdA	isocitrate dehydrogenase gene
Kan^R	kanamycin resistant
kDa	kilo Dalton
LB	Luria-Bertani Broth
LUX	Light Upon Extension
mdh	malate dehydrogenase gene
MM	Minimal Media A
MOPs	3-(N-morpholino) propanesulfonic acid
MOPS	3-(N-morpholino) propanesulfonic acid
mRNA	messenger ribonucleic acid
NADH	nicotinamide adenine dinucleotide
ndh	NADH dehydrogenase II gene
NMR	nuclear magnetic resonance
OAA	oxaloacetic acid
ompF	outer membrane protein F precursor gene
PAP1	poly(A) polymerase
Pck	phosphoenolpyruvate carboxykinase
PCR	Polymerase chain reaction
PCS	PCS scintillation fluid
PEP	phosphoenolpyruvate
pH_i	intracellular pH
phoR	Phosphate regulon sensor gene
Pi	phosphate
poly-P	Inorganic polyphosphate
ppGpp	guanisine tetraphosphate
ppk	polyphosphate kinase gene
Pps	Phosphoenolpyruvate synthase
Pro	proline
psi	force per square inch
PTS	phosphotransferase system
Pyr	pyruvate
qPCR	quantitative PCR

R^2	a measure of goodness-of fit of linear regression
RelA	GTP pyrophosphokinase
RNA	ribonucleic acid
RNP	ribonucleic acid polymerase
rpm	revolutions per minute
rpoD	RNA polymerase sigma factor D (σ^{70}) gene
RpoS	RNA polymerase stationary phase sigma factor (σ^{S}) gene
rrn	ribosomal RNA gene
Rsd	regulator of sigma 70
RT	Reverse transcriptase
RT-PCR	Reverse transcriptase PCR
RT-rtPCR	Reverse transcriptase real time PCR
SpoT	(p)ppGpp pyrophosphohydrolase
Suc	succinate
sucA	2-oxoglutalate dehydrogenase E1 component gene
sucB	dihydrolipoamide succinyltransferase component E2 gene
sucD	succinul-CoA synthetase α chain gene
Taq	*Thermus aquaticus* DNA polymerase
TBE	Tris-Borate-EDTA
TCA	Trichloroacetic acid
Tet^R	tetracycline resistant
thi-1	Unmapped mutation in thamine biosynthesis operon at 90.4 map units on chromosome: thiamine auxotrophy.
topA	DNA topoisomerase I gene
Tris	Tris-(Hydroxymethyl)amino ethane
UDG	uracil DNA glycosylase
X-gal	5-Bromo-4-chloro-3inodlyl-β-D-galactopyranoside
yhiF	ORF, hypothetical protein gene
α/β	alpha and beta
$\Delta \mu H^+$	proton electrochemical gradient
σ	sigma subunit of RNA polymerase

CHAPTER ONE

1.0 Introduction

1.1 Overview

Unicellular microorganisms such as *Escherichia coli* have the ability to detect changes in their environment and to adapt their metabolism rapidly to external fluctuations. One of the frequent changes is that of nutrients acting as a limiting factor during starvation until an adequate food source becomes available. Prokaryotes monitor their surroundings directly by membrane-bound sensors, and indirectly by intracellular sensors, which detect changes in pools of intracellular metabolites that vary as the consequence of extracellular changes. These sensors are linked through complex signal transduction pathways to global regulatory networks (Lynch and Lin, 1996). Global control systems regulate metabolic networks and one such example is carbon source utilisation. *Escherichia coli* can utilise a variety of carbon sources by regulating appropriate networks of gene, transport systems and enzymes (Jahreis and Lengeler, 1993).

The mechanisms of utilisation and transport of sugars across the bacterial cell membrane under different environmental conditions are still not completely understood (Lengeler, 1993). However, different studies have shown that prokaryotes carry a battery of carbohydrate transport systems, of which at least seven different types have been described (Fonyo *et al*., 1976). Each of these systems is optimised for specific growth conditions and depends on the energy status of the cell. Many known routes of carbohydrate uptake occur through active transport systems (Krulwich, 1990). The energy source for transportation may be transmembrane electrochemical gradients of protons (carbohydrate-H^+ symporters) (Kaback, 1990) or of sodium ions (carbohydrate-

Na^+ symporters) (Dimroth, 1990), hydrolysis of ATP (Ames, 1990), or vectorial transport (Meadow *et al.,* 1990; Saier and Chin, 1990).

Glucose is the primary sugar used by many prokaryotes as a carbon source. In the absence of glucose, the cell resorts to other carbon sources to generate glucose (Brosnan, 1999*). De novo* synthesis of glucose from lipids and amino acids is termed gluconeogenesis. Amino acids, lipids and other gluconeogenic substrates are generally degraded to Krebs cycle intermediates prior to gluconeogenesis.

1.1.1 Gluconeogenesis

Gluconeogenesis, the reverse of glycolysis, is a universal process occurring in most living organisms (Fig. 1). Both the glycolytic and gluconeogenic pathways are independently regulated via reactions that are specific for either pathway. However, many steps are shared between these two processes. Although most of the gluconeogenic reactions are the reverse of glycolysis reactions, three steps in glycolysis are irreversible. They are; the conversion of glucose to glucose-6-phosphate; the conversion of fructose-6-phosphate to fructose-1,6-bisphosphate, and the conversion of phosphoenolpyruvate (PEP) to pyruvate.

1.1.2 Gluconeogenesis in Escherichia coli

For gluconeogenesis, three irreversible reactions are important in *E. coli* K12 (Sanwal, 1970): Phosphoenolpyruvate carboxykinase (Pck) which converts oxaloacetic acid (OAA) to phosphoenolpyruvate (PEP); phosphoenolpyruvate synthase (Pps) which converts pyruvate to PEP, and fructose-bis-phosphatase (Fbp) which converts fructose-

1,6-bisphosphate to fructose-6-phosphate (Fig. 1). The enzyme responsible for the first committed step of gluconeogenesis from Krebs cycle intermediates is Pck.

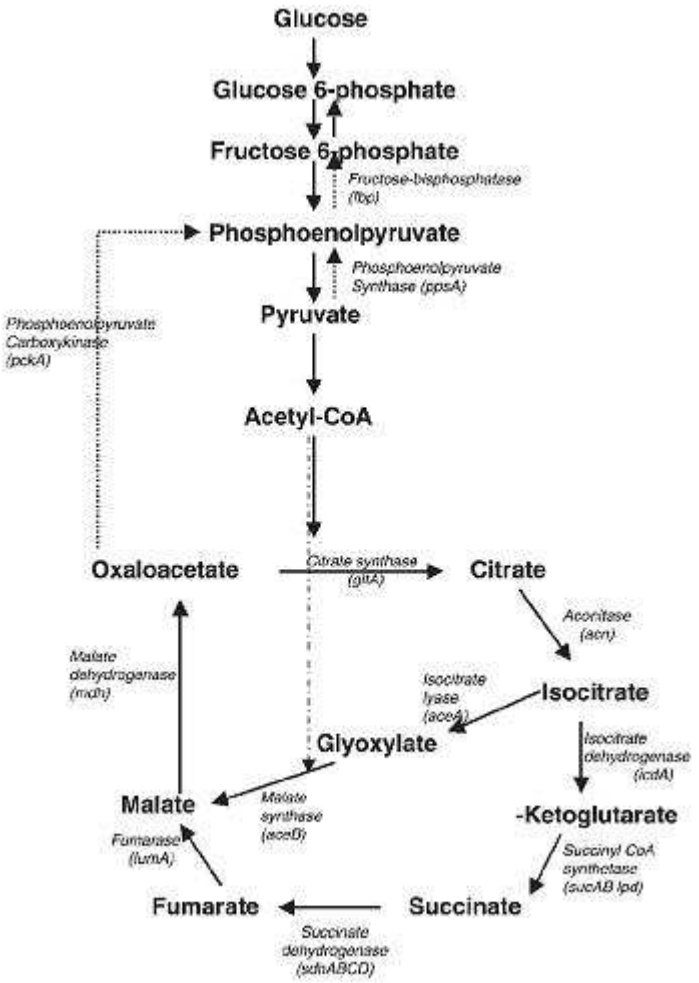

Fig 1: Pathways of carbohydrate metabolism in *Escherichia coli*. Genes are named in parentheses. Adapted from Phue *et al.,* 2005.

At the onset of stationary phase, bacteria convert carbohydrate to glycogen used for storage of energy (glycogenesis). Pck activity and gluconeogenesis are therefore required to produce carbohydrates if they are not present in the growth medium. A key regulatory gene involved in glycogenesis is known as *csrA* (carbon storage regulator) (Romeo *et al.*, 1993). It negatively controls *glgC* and *glgB* (genes for enzymes involved

in glycogen synthesis) as well as the genes expressing gluconeogenic enzymes like *pckA* (Sabnis *et al.,* 1995). However, the effect of *csrA* is not large enough to explain stationary phase induction of *pckA* (Goldie, 1984). The conversion of carbohydrate into endogenous glycogen is favoured as the cells enter stationary phase, while in late stationary phase, there is a decrease in activities of the gluconeogenic enzymes (Sabnis *et al.,* 1995).

Carbohydrate metabolism also plays a critical role in anaplerosis, which is the replenishing of Krebs cycle intermediates. Gluconeogenesis could be viewed as a catapleurotic reaction, where the Krebs cycle intermediates are depleted by withdrawing oxaloacetic acid from the Krebs cycle to produce PEP (Brosnan, 1999). Gluconeogenesis may occur only when balanced by anapleurotic reactions like synthesis of four carbon units by the glyoxylate pathway or by the production of intermediates from gluconeogenic amino acids. In the presence of some carbohydrates, the gluconeogenic pathways in prokaryotes are subjected to catabolite repression. In the absence of carbohydrates, high levels of cAMP will activate the transcription of genes encoding gluconeogenic enzymes. Gluconeogenesis is also important when the bacteria have depleted most of the carbohydrate in the medium and they have to rely on gluconeogenesis for the synthesis of glucose from amino acids and fats for growth.

1.1.3 Synthesis of phosphoenolpyruvate (PEP)

Two pathways exist for the synthesis of PEP from four-carbon intermediates in *E. coli* during gluconeogenesis. One pathway involves the enzyme Pck while the other involves the sequential action of the NAD-dependent malic enzyme and Pps ((Fig. 1),

Goldie and Sanwal, 1980). Gluconeogenic growth in *E. coli* is controlled by *pck* and *pps* as determined by Goldie and Sanwal, (1980a) and Chao *et al.* (1993).

For growth on succinate and other four carbon metabolites, Pck converts oxaloacetate to PEP, which can be converted to pyruvate by pyruvate kinase (Chao *et al.,* 1993). Mutants with null alleles of *pps* cannot grow on pyruvate (Cooper *et al.,* 1967) but can grow on succinate (Fig. 1). To generate a Suc^- phenotype (inability to grow on succinate minimal medium), null alleles in both *pps* and *pck* are needed since malic enzymes and Pps can supply PEP in pck^- cells (Goldie and Sanwal, 1980a). Double mutants, deficient in Pck and Pps or double mutants deficient in Pck and the NAD-dependent malic enzyme are unable to grow on four carbon sugars such as succinate, fumarate, malate, acetate and pyruvate but grow well on glucose or glycerol as a sole carbon source. On the other hand, single mutants deficient in any of these enzymes are able to grow on four-carbon intermediates readily (Goldie and Sanwal, 1980a).

Although two pathways were shown to exist for the synthesis of PEP during gluconeogenesis in *E. coli*, our focus will be on the major pathway, Pck. The gene coding for Pck (*pckA)* appears to have interesting regulatory mechanisms, since it is regulated genetically by catabolite repression and activated by another unknown signal in stationary phase (Goldie, 1984).

1.2 Phosphoenolpyruvate carboxykinase (Pck) in *Escherichia coli*.

1.2.1 Structure of Pck

E.coli Pck is a monomeric, globular protein of Mr 60,000 that belongs to the α/β class of proteins. It has two domains, a 275 amino acid residue N-terminal domain and a

compact 265 amino acid residue C-terminal domain. The active site is found at the base of a deep cleft between the two domains (Sudom *et al.*, 2003).

The crystal structure of the ATP-Mg^{2+}-Ca^{2+}-pyruvate-Pck quinary complex of *E. coli's* Pck was solved using molecular replacement techniques (Sudom *et al.,* 2003) and the structure was subsequently refined against 1.8-Å resolution data. This structure is isomorphous to that of the ATP-Mg^{2+}-Mn^{2+}-pyruvate Pck complex (Tari *et al.,* 1997) except for the Ca^{2+} and Mn^{2+} binding sites. Under the crystallisation conditions, ADP and PEP react to form ATP and pyruvate. In the presence of saturating concentration of ATP, Pck requires divalent metal cations for activity. Kinetic studies on ATP demonstrate that combinations of Mg^{2+} and Mn^{2+} or Mg^{2+} and Ca^{2+} induce synergistic activations of enzyme activity, suggesting a dual cation function (Goldie and Sanwal, 1980b). X-ray crystallography (Tari *et al.,* 1997) shows that both metals are present at the active site. Optimum activity was observed in presence of millimolar concentration of Mg^{2+} and micromolar concentrations of Mn^{2+} (Goldie and Sanwal, 1980b). When MgATP binds, Pck undergoes a domain closure via a 20-degree rotation of the amino and the carboxyl terminal domains towards each other. This traps substrates, excludes solvent from the active site and repositions the important active site groups and metal ions in the active site. When Mg^{2+} is absent, there is no synergistic effect of adding Ca^{2+} and Mn^{2+}. The synergistic effect of adding Ca^{2+} can be abolished by partial digestion of Pck by trypsin while this does not affect Mn^{2+} activation. Binding of the fluorescent Ca^{2+} analogue, Tb^{3+} indicates the presence of two Tb^{3+} sites on Pck (Goldie and Sanwal, 1980b) while the X-ray crystallography structure of $(Tb^{3+})_2$ complex of Pck showed the possibility of Ca^{2+} as an allosteric regulator of Pck via binding at both an internal active site and at a surface activating site (Matte *et al.,* 1996). In 2003, Sudom, *et al.,* were able

to solve the crystal structure of the ATP-Mg^{2+}-Ca^{2+}-pyruvate quinary complex of Pck. They showed that Pck complex contains Ca^{2+} at the active site and not at the putative allosteric site; however as mentioned, partial digestion of Pck can abolish activation by Ca^{2+} without affecting activation of Mn^{2+} (Goldie and Sanwal, 1980b). Thus, Mg^{2+} and Ca^{2+} both possess two distinct binding sites. Mg^{2+} correctly positions and activates ATP while Ca^{2+} (or Mn^{2+}) serves to activate the Pck catalytic reaction by directly bridging and activating ATP and the enolate anion of pyruvate. The chemical properties of Ca^{2+}, observed changes in active site residues and substrate orientation as well as studies of mutant Pcks indicate that Ca^{2+} may serve as a non-allosteric activator in dual metal ion-facilitated phosphoryl transfer.

1.3 Regulation of genes in stationary phase.

Stationary phase is a general stress response that leads to dramatic changes in the protein profile and cellular composition and metabolism, which increase the cell's resistance to many different harmful conditions. Transcription in bacteria is performed by a single multisubunit RNA polymerase (RNP). Core RNP is capable of transcript elongation but not of promoter-specific transcript initiation. For initiation to occur, it requires the addition of a sigma subunit (σ) to form the holoenzyme that is competent for promoter recognition and the formation of transcriptionally competent "open" complexes. The core enzyme has a subunit composition of $\alpha_2\beta\beta'\omega$ and a mass of 389 kDa (Busby and Ebright, 2000). A sigma subunit directs the core enzyme to initiate transcription at specific promoter sites on DNA. *E. coli* uses at least seven different σ factors. The gene expression profile of an individual cell will depend on the proportions of total RNP that are bound by the different σ factors (Ishihama, 2000). Changes in σ

factor activity provide an important mechanism for bacteria to respond to their environment. The activity of most σ factors is determined by their cellular level and also by the activity of anti-σ factors that prevent cognate σ factors from interacting with RNP (Dove *et al.,* 2000). Most attention has focused on σ^{70}, the product of the *rpoD* gene, the most abundant σ factor that enables *E. coli* RNP to recognise most promoters and to initiate transcription (Ishihama, 2000; Murakami and Darst, 2003). During exponential cell growth, σ^{70} is responsible for transcription of most genes. However, when the cell enters stationary phase, the central regulator of stationary phase transcription is the sigma factor RpoS (σ^{38} or σ^{s}) whose accumulation is responsible for the expression of scores of stationary phase-specific genes (Hengge-Aronis, 2002). Most of these genes encode proteins that assist survival during stationary phase. Transcription of many of these genes is dependent on RpoS and thus these genes are not expressed during logarithmic growth.

Although RpoS is considered to be the stationary phase sigma factor in *E. coli*, σ^{70} still remains the predominant σ factor during stationary phase (Jishage and Ishihama, 1995). A non-growing cell "is believed" to have twice as many σ^{70} molecules as RpoS molecules (Ishihama, 2000; Jishage and Ishihama, 1995). Also, it has been shown that RNP has a higher affinity for σ^{70} than for RpoS (Maeda *et al.,* 2000; Colland *et al.,* 2002). The question of how RpoS can capture sufficient RNP to assure the expression of the essential RpoS-dependent genes still needs to be addressed. Jishage and Ishihama (1998) came to one possible explanation. They were able to identify an *E. coli* protein consisting of 158 amino acids residues, which is expressed upon entry into stationary phase and that can bind to σ^{70} but not to RpoS. *In vitro* and *in vivo* studies with this protein suggested that it inhibits the transcription of σ^{70}-dependent promoters (Jishage

and Ishihama, 1998; 1999). This protein and its corresponding gene were named Rsd (regulator of σ^{70}) and *rsd* respectively. Subsequent biochemical studies showed that Rsd could contact the carboxyl-terminal domain of σ^{70} (Jishage *et al.,* 2000). Further mutational analyses identified σ^{70} residues located at a conserved region of domain 4, that contacts -35 elements at promoters and many trans-acting factors, to be important for the interaction with Rsd (Dove and Hochschild, 2001). To probe further the extent of the Rsd contact site on σ^{70}, Westblade *et al.,* (2004), studied Rsd and σ^{70} and were able to show that Rsd and σ^{70} formed a 1:1 complex. Moreover, Rsd inhibited the core binding activity of σ^{70} domain to RNP by binding to some of σ^{70} side chains located in the 4.2 region (conserved region of domain 4 that contacts -35 elements at promoters and many trans-acting factors), thus confirming that region 4.2 is a crucial point of contact between Rsd and σ^{70} (Westblade *et al.,* 2004). Thus, the presence of Rsd during the stationary phase led to the suggestion that its principal role is simply to sequester σ^{70} in nongrowing cells, so that more core RNA polymerase could be "captured" by the alternative factor, σ^{38}, which is needed for the expression of certain genes important for nongrowing cells.

Sequence alignments (Becker and Hengge-Aronis, 2001; Espinosa-Urgel *et al.,* 1996; Lee and Gralla, 2001) as well as *in vitro* selection of an optimized RpoS-driven promoter (Gaal *et al.,* 2001), demonstrated that the –10 region consensus is identical for RpoS and σ^{70} dependent promoters. The difference lies in observations made by many studies, which showed that RpoS-dependent promoter sequences always have high conservation of the –10 promoter element, whereas the –35 element tends to be more degenerate than in σ^{70}-dependent promoters (Becker and Hengge-Aronis, 2001; Espinosa-Urgel *et al.,* 1996; Lee and Gralla, 2001). This is consistent with the

observation that *in vitro*, the RNP core enzyme/RpoS promoter interaction focuses on the –10 region, whereas contacts with the –35 region can be weak (Colland *et al.,* 1999) thus RpoS-containing RNP can use degenerate –35 regions more efficiently that RNP core enzyme σ^{70}. From these observations, it was concluded that some promoters could be recognized by both RpoS and σ^{70} while others are recognized only by one of those sigma factors (Tanaka *et al.,* 1997).

In *E. coli*, *rpoS* expression is modulated at the level of transcription, translation and post-translational stability (Bertani *et al.,* 2003). In *E. coli*, different stress signals control RpoS at the translational level via RNA regulatory molecules (dsrA, oxyS, rprA), secondary RNA structure, and RNA binding proteins (HU, H-NS and Hfq) (Hengge-Aronis, 2002). DsrA and rprA activate *rpoS* translation (Sledjeski *et al.,* 1996), while OxyS inhibits RpoS translation by binding Hfq in competition with the *rpoS* leader (Zhang *et al.,* 1998). The RNA-binding histone-like protein H-NS, has been implicated in negative translational regulation of RpoS levels (Barth *et al.,* 1995; Yamashino *et al.,* 1995), while RNA binding protein Hfq increases translation of *rpoS* mRNA since *hfq* mutants have shown to have a reduced level of RpoS (Brown and Elliot, 1996; Muffler *et al.,* 1996).

Post-translationally, RpoS levels are controlled through its degradation by a response regulator called RssB and the ClpXP protease (Zhou and Gottesman, 1998). The increase in RpoS levels in stationary phase results in part from a substantial increase in its stability. The instability of RpoS during exponential growth phase is due to the activity of the ClpXP protease, which recognises a 20 amino acid stretch between residues 170 and 190 (Schweder *et al.,* 1996). This degradation is stimulated by the response regulator RssB (or SprE) (Muffler *et al.,* 1997c, Pratt and Silhavy, 1996),

which increases the rate of ClpXP proteolysis by interacting with RpoS forming a complex that reduces activity of RpoS (Zhou and Gottesman, 1998). The decrease in degradation of RpoS in stationary phase is not due to a decrease in ClpXP but rather due to the presence of chaperone DnaK, which is ascribed the role of protecting RpoS from ClpXP (Muffler *et al.,* 1997a; Rockabrand *et al.,* 1998).

Transcriptional regulation of *rpoS* in *E. coli* also occurs but it appears to be less important (Venturi, 2003). A two-component sensor called BarA/UvrY, cAMP, and molecules such as polyphosphate and ppGpp (guanosine 3',5'-bis pyrophosphate) have been implicated in transcriptional regulation of *rpoS* (Hengge-Aronis, 2002). The BarA sensor kinase has been demonstrated to induce *rpoS* transcription. In a *barA* mutant, it has been found that the amount of *rpoS* mRNA as well as RpoS protein are decreased (Mukhopadhyay *et al.,* 2000). Afterwards, BarA was shown to be a cognate kinase of UvrY, a response regulator of the FixJ family (Pernestig *et al.,* 2001). Surprisingly, UvrY does not seem to be implicated in *rpoS* activation (Hengge-Aronis, 2002b) and thus suggests that BarA activates *rpoS* through a different and unknown response regulator. Hence, BarA and UvrY could both be involved in the regulation of *rpoS* levels but in different ways: BarA upregulates *rpoS* whereas UvrY has a negative effect (Oshima *et al.,* 2002). Moreover, we do not know if Bar A and UvrY are mutually dependent on each other to bring about these different controls and the signals that modulate this two-component system have yet to be determined (Oshima *et al.,* 2002).

The *rpoS* promoter of *E. coli* contains two putative cAMP-Crp binding sites (Hengge-Aronis, 2002b). Transcription of a *rpoS-lacZ* fusion was reported to increase in the exponential phase of growth in *cya* (adenylate cyclase) and *crp* mutants, suggesting that the cAMP-Crp complex is involved in transcriptional repression rather than its

classical role as an activator (Lange and Hengge-Aronis, 1994). The observation that a *crr* knockout mutant demonstrated a de-repressed expression of *rpoS* and accumulated 20 times more RpoS in exponential phase is consistent with a role for cAMP-Crp as a negative regulator (Ueguchi *et al.,* 2001). A vital component of the phosphophenolpyruvate carbohydrate phosphotranferase system (PTS) of glucose uptake is Crr protein. It is also a regulator of several cellular functions, including the modulation of cAMP synthesis (Ueguchi *et al.,* 2001). In fact, if cAMP is added in mid-exponential phase to a *crr* mutant containing a *rpoS-lacZ* transcription fusion, the wild type level of *rpoS* can be restored. This observation indicates that Crr acts indirectly probably through modulating cAMP levels (Ueguchi *et al.,* 2001).

In *E. coli* and *Pseudomonas,* the involvement of the ppGpp as a positive signal of *rpoS* expression has been reported (Gentry *et al.,* 1993; Hirsch and Elliott, 2002). The ribosome associated RelA protein synthesised ppGpp due to a physiological response to nutritional stress. Under starvation conditions, SpoT also mediate the synthesis of ppGpp. Thus, only *spoT relA* double mutants completely lack ppGpp. Activity of *rpoS-lacZ* fusions and RpoS levels are reduced in *E. coli spoT relA* double mutants. This decrease have been attributed not to lower transcription initiation but to reduced elongation by promoter deletion studies. This could be due to premature transcriptional termination caused by the uncoupling of transcription and translation (Lange *et al.,* 1995). ppGpp also increases RpoS levels at the post-transcriptional level as demonstrated by measuring the rate of RpoS synthesis by pulse labeling. ppGpp seems to induce translation indirectly by regulating a non-ribosomal factor necessary for *rpoS* translation (Brown *et al.,* 2002).

The ppGpp "alarmone" has a positive control on the accumulation of inorganic polyphosphate (Gentry *et al.,* 1993). Inorganic polyphosphate (poly-P) is a linear molecule that consists of hundreds of orthophosphate residues that accumulates in many bacteria under stress conditions and in stationary phase. It is a form of energy storage and has an important role in regulatory responses (Kornberg *et al.,* 1999). Polyphosphate kinase is encoded by the *ppk* gene and polymerizes the terminal phosphate of ATP into a poly-P chain. The *ppx* gene encode exopolyphosphatase, poly(P)ase and degraded poly-P. In *E. coli*, if the amount of poly-P is reduced to barely detectable levels by over expressing a *ppx* gene, then significant decrease in *rpoS-lacZ* transcription would be observed. Under these conditions, RpoS levels fail to increase upon entry into stationary phase (Shiba *et al.,* 1997).

1.4 *pckA* gene encoding PEP carboxykinase

The gene encoding the enzyme Pck in *E.coli* K12 is the *pckA* gene. Medina *et al*. (1990) sequenced the gene and mapped one strong mRNA start site using the S1 nuclease method. They were able to identify potential transcriptional regulatory sequences. Expression of *pckA-lacZ* operon fusions is induced in stationary phase cells (Goldie, 1984). Transcription of *pckA* appears to be controlled by a 280 bp region between a *Cla I* site and the initiation codon (Fig.2). A strong sigma σ^{70} promoter is located at –10 and –35 positions (Medina *et al.,* 1990). N-terminal sequences of the enzyme and proteolytic fragments were used to confirm the identity of the protein product and the position of translational start. There is a 140 bp leader region between the transcription and translation start sites of unknown function (Fig.2).

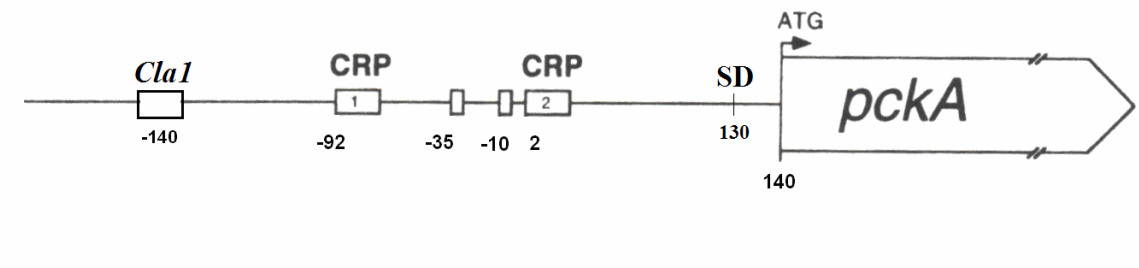

Fig 2: Promoter region of *pckA*. CRP is the Crp binding site, -35 and -10 represent the binding site of σ^{70} and SD represents the Shine Delgarno ribosomal binding site. Between the transcriptional and translational start site there is a 140 bp leader region.

1.4.1 Regulation of pckA expression in Escherichia coli.

Cyclic AMP receptor protein (Crp) and 3',5'-cyclic AMP (cAMP) are global regulators in carbon utilisation and play an important role in catabolite repression. This occurs because transport of glucose by the phosphotransferase system (PTS) diminishes activation of adenylate cyclase by factor IIA glucose phosphate and thus represses the formation of enzymes, such as Pck, whose activities would increase the already large intracellular pools of glycolytic metabolites. Catabolite repression probably serves the purpose of inhibiting gluconeogenesis when glucose and other carbohydrate carbon sources are available. Crp binds to cAMP forming a cAMP-Crp complex, which binds to specific sites at or near target promoters and brings about activation of transcription. (De Crombruggh *et al.,* 1984). Crp is encoded by the *crp* gene, while adenylate cyclase (cAMP synthesis) is encoded by *cya* gene. Gel shift experiments indicated that three molecules of Crp protein bound to the *pckA* promoter in the presence of cAMP while footprints have been obtained for two of these sites, *Crp1* and *Crp2* (Goldie, unpublished). In 1984, Goldie *et al.,* used Mud(*lacZ* Amp^R) bacteriophage to isolate

operon fusions of the transcriptional control sites of *pckA* to the β-galactosidase structural gene (*lacZ*), which showed that stationary-phase induction is probably exerted at the transcriptional level. The fusions were induced up to 100-fold at the onset of stationary phase in cells grown on LB while levels of β-galactosidase were lowered when glucose was added (Fig.3). On LB medium, β-galactosidase synthesis was not induced in *pckA-lacZ* fusions until the onset of stationary phase; although cAMP levels were high throughout growth. The fusions did not express high β-galactosidase activity during log-phase when cells were growth on LB with 5 mM cAMP (Fig.4). It was concluded that Pck synthesis is regulated not only by cAMP and glucose, but also by another unknown regulatory signal which is either required to inhibit *pckA* expression during log phase or to induce *pckA* expression during stationary phase.

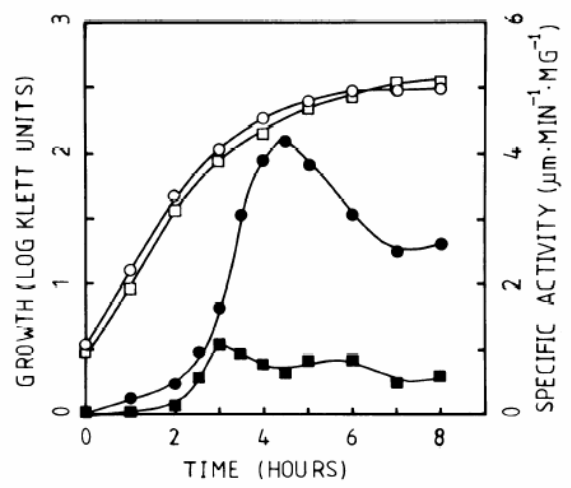

Fig. 3: Growth (log optical density in Klett Units) and β-galactosidase specific activity were plotted for *pck-lacZ* fusion strain grown on LB in the presence and absence of glucose. Open circles are growth on LB and black circles are β-galactosidase specific activity. Open squares represent growth on LB + 0.4% glucose and black squares represent β-galactosidase activity in the presence of glucose and LB. Adapted from Goldie, 1984.

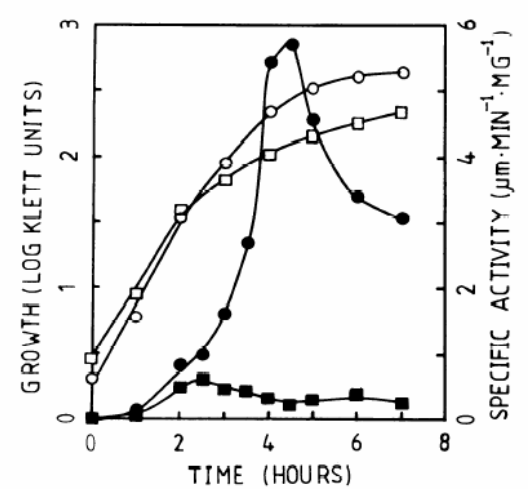

Fig. 4: Growth and β-galactosidase specific activity for *cya pckA-lacZ* fusion strain grown on LB in presence or absence of 5mM exogenous cAMP. Open squares represent growth on LB and black squares represent β-galactosidase specific activity for cells grown on LB only. Open circles represent growth on LB + 5mM cAMP while black circles represent β-galactosidase specific activity for cells grown on LB + 5mM cAMP. Adapted from Goldie, 1984.

Besides cAMP, Ramseir *et al*. (1995) reported that the fructose repressor FruR (which is known to regulate expression of several genes concerned with carbon utilisation), also controls the expression of *pckA*. However, Goldie (unpubished) has been unable to observe an effect of *fruR* mutations on Pck activity. A putative FruR operator site was reported about 100 bp upstream from the -35 promoter region of *pckA* Ramseir et *al.,* 1995; (Fig. 5). FruR has also been found to bind to a target DNA region located around -45.5 upstream of the *ppsA* gene and circular permutation analysis showed that upon binding to its site, FruR induces a sharp bend of 120^{o} in the DNA helix suggesting a crucial involvement of FruR-induced bending in *ppsA* promoter activation (Negre *et al.,* 1998).

Using computer analysis to study the prevalence of DNA static curvature in regulatory regions of *E. coli*, Olivares-Zavaleta *et al.,* (2006) reported that the FruR regulator has a tendency to regulate operons with curved sequences in their 5' upstream regions.

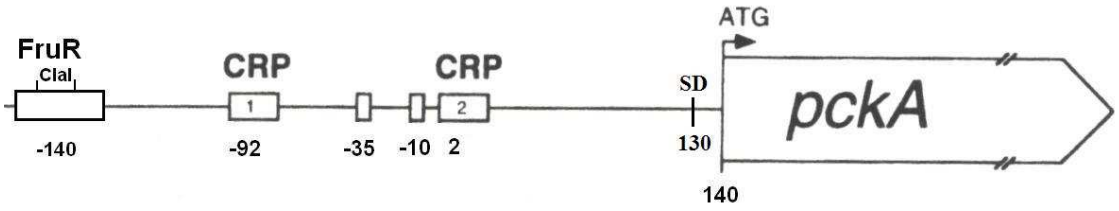

Fig. 5: Diagramatic representation of potential FruR binding site, which is located around 100 bp upstream of the -35 promoter binding site (Ramseir *et al*., 1995).

1.5 ATP synthase in *Escherichia coli*

ATP synthase (ATPase) has a molecular mass of 520,000 daltons (Capaldi and Schulenberg, 2000). It is a multisubunit enzyme which catalyses the synthesis of ATP from ADP and phosphate (P_i), utilising energy derived from the proton electrochemical gradient (ΔH^+) formed by electron transport (Hazard and Senior, 1993). It is a reversible H^+ pump, which plays two metabolically defined roles: in aerobic conditions, it utilises the proton motive force from the respiratory chain to synthesise ATP, and in anaerobic conditions, it utilises ATP from glycolysis to pump protons out of the cell, forming an electrochemical H^+ gradient that supplies energy for secondary transport systems (Shin *et al.,* 1992). Wild type *E. coli* can use both oxidative phosphorylation and substrate level phosphorylation, whereas *atp* mutants (defective in ATPase) are dependent mainly on substrate level phosphorylation (Jensen and Michelsen, 1992).

1.5.1 Structure of ATP synthase

ATPase consists of eight different subunit types, in stoichiometry $\alpha_3\beta_3\gamma\delta\varepsilon ab_2c_n$. (Weber *et al.,* 2004). These subunits are divided into the catalytic core (also known as the F_1 region) which consists of $\alpha_3\beta_3\gamma$, the stalk [rotor ($\varepsilon\gamma$) and stator ($b_2\delta$)] and the

proton transport unit (also know as the F_0 region) ac_n (Fig. 6). Proton transport is effected by *a* and *c* subunits (Fillingame *et al.,* 2000; Kaim *et al.,* 1998; Rastogi and Girvin, 1999). The "rotor stalk" composed of εγ, is connected firmly to the *c*-ring at the base, and interacts with α and β at the top (Nakamoto *et al.,* 1999; Stock *et al.,* 1999; Capaldi *et al.,* 2000). The movement of protons is believed to generate rotation of subunits *c,*ε and γ which act on the catalytic site (Diez *et al.,* 2004). The catalytic core of the enzyme consists of a hexagon of alternating α and β subunits with helices of γ in the centre. ATP synthesis and hydrolysis reactions occur at three catalytic sites (Leslie and Walker, 2000).

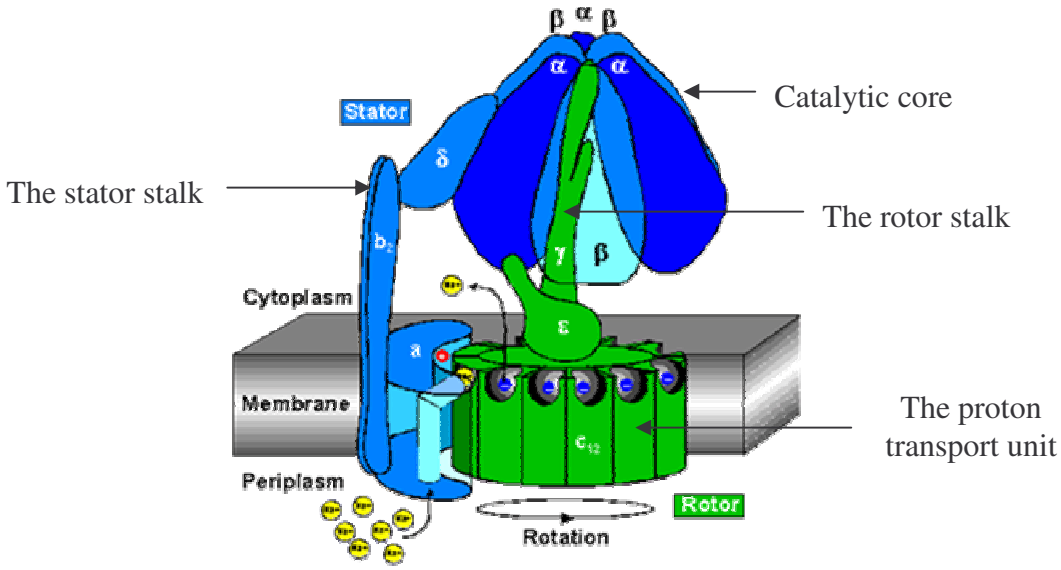

Fig. 6: A diagrammatic representation of ATPsynthase. Adapted from (www.micro.biol.ethz.ch/op/ op_semdipl_dimroth2.htm)

The three catalytic sites are located at the α/β interfaces of the alternating α/β hexagon (Hausrath *et al.,* 1999). The γ-subunit shows three different faces, one to each α/β catalytic site interface, and is widely assumed to thereby impose a different

conformation on each catalytic site (Weber and Senior, 2000; 2001; Nadanaciva *et al.,* 2000). The stator is important to resist the rotor strain. The "stator stalk" is composed of $b_2\delta$, with δ contacting an α-subunit at the top of the molecule (Wilkens *et al.,* 2000; Ogilvie *et al.,* 1997), and b_2, anchored in the membrane by the N-terminal transmembrane helices (Dmitriev *et al.,* 1999). The *b* subunit interacts with the *a*-subunit in the membrane (McLachlin *et al.,* 2000; Jiang and Fillingame, 1998). The F_0 portion in the membrane functions as a proton-driven motor that allows passive proton translocation caused by a proton gradient across the membrane. Subunit *c* functions as a rotor in the F_0 region. It rotates relative to the ab_2 complex, powered by the energy generated by the electron motive force across the membranes (Fillingame *et al.,* 2002) in which H^+ ions are believed to be transferred through aqueous channels of subunit *a via* a carboxyl-group of subunit *c* (*c*Asp61 in *Escherichia coli*). NMR study of *E. coli* subunit *c* (EF_0c) has revealed a hairpin-shaped conformation of subunit *c* (consisting of 10-14 residues), with two α-helices (Dmitriev *et al.,* 1999). During catalysis, the subunit *b* dimer undergoes transient elastic deformation in order to compensate for the torque which is built up by the propelling rotor (Capaldi and Aggeler, 2002). This torque is released by conformational changes leading to either H^+ pumping through F_0 or ATP synthesis in F_1. The molecular switch, by which one or the other direction of catalysis is preferred, has been attributed to the ε subunit (Schulenberg *et al.,* 1997). From the studies so far, two models have been proposed for the rotation (or torque generation) mechanisms of the F_0 motor (Nakano *et al.,* 2006). The first one relies on simple rotational diffusion of the *c*-ring, which is driven by electrostatic forces across the membranes. This model assumes a rigid *c*-ring structure (Dimroth *et al.,* 2003). The

structure of the *c*-ring from *I. tartaricus* Na^+-ATPase seems to support the model. This model is proposed to work for Na^+ pumping. The second model is more mechanical. A protonation-linked conformational change within subunit *c* drives larger-scale rotations of the whole *c*-ring in this model, derived from NMR observations (Rastogi and Girvin, 1998). Taking the twist motion into consideration, this model is consistent with cross-linking results between *a-c* subunits, (Jiang and Fillingame, 1998) and between *c-c* subunits (Jones *et al.,* 1993). On the other hand, a double mutation experiment showed that the aspartate residue (*c*Asp61 in *E. coli*) can be relocated to the neighboring N-terminal helix without loss of function (Miller *et al.,* 1990). This result implies that a global conformational change in the C-terminal helix of subunit *c* is not necessarily required for proton translocation.

1.5.2 Genetic mapping of atp genes

Each subunit of ATPsynthase is encoded by a single gene in the operon (Walker *et al.,* 1984). The order of the genes in the operon is *atpB, atpE, atpF, atpH, atpA, atpG, atpD* and *atpC*, that encode the subunits *a, c, b,* δ, α, γ, β, and ε respectively. The *atp* operon maps at 84.6 min on the *E. coli* chromosome. A promoter sequence 73 bp upstream of *atpB* has been identified (Gay and Walker, 1981) and confirmed by the study of Tn*10* insertions (Von Meyenburg *et al.,* 1982) and Dnase I footprinting studies. Porter *et al.,* (1983) showed that the promoter 73 base pairs upstream of the open reading frame is strongly active both *in vivo* and *in vitro* and it was concluded to be the *atp* promoter since the other promoter-like sequences upstream of *atpB* were either inactive or weakly active. They also concluded that the open reading frame preceding

the *atpB* is part of the *atp* operon and they named it *atpI*. The *atpI* gene product appears to be a hydrophobic protein. The *atp* operon expression was shown to occur from a single promoter located immediately before *atpI* (Kasimoglu *et al.,* 1996). They also suggested that the cell growth rate, rather than the type of carbon compound used for growth, is the major variable in controlling *atp* gene expression.

1.6 Research Objectives

1.6.1 Previous findings

The *pckA* gene is regulated at the transcriptional level by cAMP and requires another unknown regulatory signal for its induction at stationary phase (Goldie, 1984). Madhavan (2002) found that mutations in *atpG* encoding ATP synthase could lower the expression of *pckA* in *E.coli*. Stationary phase sigma factor σ^{38}, encoded by *rpoS* has been found to induce around 100 genes (Venturi, 2003). The first objective of Madhavan was to determine the effect of *rpoS* on *pckA*. She transduced *rpoS*::Tn*10* into a *pck-lacZ* strain and found that there was no effect of the *rpoS*::Tn*10* on the transcriptional fusion since all the transductants had the same blue colour on X-gal plates and there was no difference in β-galactosidase activities in *pck-lacZ* fusions in *rpoS*$^{+}$ or *rpoS*$^{-}$ strains. Other stationary phase regulators such as *glnG, relA* (nitrogen limitation), *phoR* (phosphate limitation), and oxygen limitation were already ruled out (Goldie and Sanwal, 1980a). Madhavan performed mutagenesis using MiniTn*10*-ATS [(Kleckner *et al.,* 1991), a kanamycin resistance transposon which lacks a transposase gene giving it more stability and less target specificity, to isolate mutants from strain HG163 (*pps*$^{-}$ and *pckA*$^{+}$). She was able to isolate seven mutants with low specific activity of Pck (Pck^{-}) and slow growth rate (Gro^{-}). She investigated further to find a relationship between these two phenotypes. In *recA* mutants she found that, growth rate as well as growth yield was low (Gro^{-}) while Pck specific activity was similar to wild type, (Pck^{+}). In *pckA* mutants, she found that only Pck specific activity was affected (Pck^{-}) while growth rate was like wild type (Gro^{+}). Therefore, she concluded that these two phenotypes are not related to each other. Her third objective was to try to characterise the mutants she obtained. It has

been found by genetic linkage that *pckA* is linked 20-30% to *asd* (Goldie and Sanwal, 1980a). From the mutants that were isolated, she obtained four (HG203, HG204, HG205 and HG206) that were not linked to *asd* and thus the low Pck specific activity in these mutants was not due to a mutation of *pckA*. Her next step was to find if these mutants were *cya* or *crp* since previous work showed that *cya* or *crp* mutants were obtained when trying to isolate regulatory mutants of *pckA* (Chan, 1987; Goldie, unpublished results). Mutants defective in *cya* or *crp* will not ferment sugars such as maltose and arabinose since the cAMP-Crp complex is required for the activation of the *mal* regulon and *ara* operon (Plumbridge, 2001; Notley and Ferenci, 1995). If the mutations in these isolated mutants were in the *cya* or *crp* gene then they would not be able to ferment maltose and arabinose. However, these isolates (HG203, HG 204, HG205 and HG206) did ferment these sugars suggesting that the mutations, affecting *pckA* were not in the *cya* or *crp* genes. Two pathways are involved in gluconeogenesis for the synthesis of PEP. One is the conversion of pyruvate to PEP by the enzyme phosphoenolpyruvate synthase (Pps) and the other is the conversion of oxaloacetate to PEP by phosphoenolpyruvate carboxykinase (Pck) (Goldie and Sanwal, 1980a). A $pps^{+}/pckA^{-}$ mutant will grow on succinate as carbon source (Suc^{+} phenotype) because succinate is converted to malate, which in turn is converted to pyruvate by NAD dependent malic enzyme, which will be used by Pps to produce PEP, while $pps^{-}/pckA^{-}$ double mutants will not be able to grow on succinate (Suc^{-} phenotype). These four strains (HG203, HG 204, HG205 and HG206) were transduced to pps^{+} (using W3350 as a donor) to see whether the *pps* mutation was regulated for the Suc^{+} phenotype. However, the phenotype of the mutants after transduction to pps^{+} remained Suc^{-}, since there was no growth of mutants on minimal plates containing succinate. This

observation led to the conclusion that the mutations were in a gene or genes where the Suc^- phenotype is independent of expression of the *pckA* gene. Her fourth objective was to try to identify where insertion of the miniTn*10*-ATS occurred in the mutants by PCR of DNA flanking the insertion points and the observations made were surprising. The Suc^-, Gro^-, Kan^R mutants did not contain MiniTn*10*, as demonstrated by PCR. The deduction from this observation was that spontaneous mutations could have led to the formation of those mutants. It has been found by Thorbjarnadottir *et al.,* (1978) that mutations in the *atp* gene could confer resistance to aminoglycoside drugs such as kanamycin. Mutants of *atp* are also Suc^- and this could be due to uncoupling and disruption of the electrochemical gradient and to transport defects (Boogerd *et al.,* 1998). Downie *et al.,* 1980 have also shown that *atp* mutations have no effect on growth rate but affect growth yield. Madhavan's next experiment was to transform HG203, HG205 and HG206 with plasmids expressing the complete *atp* operon and she was able to get Kan^S Suc^+ phenotypes. The transformed mutants had higher Pck specific activities and higher growth yields (Gro^+). However, the Pck specific activity was not as high as wild type. Transforming the mutants with plasmids expressing the F_1 region of ATP synthase (Klionsky and Simoni, 1985), did complement the Suc^-, Kan^R, Pck^- , Gro^- and $ATPase^-$ (Atp^-) phenotypes of the three mutants. Transforming with plasmid expressing the γ subunit of ATP synthsase (Shin *et al.,* 1992) complemented the Suc^-, Gro^- and Kan^R phenotypes in mutants thus indicating that the mutation was in *atpG*. From those observations, she concluded that Suc^-, Kan^R, Pck^- , Gro^- and Atp^- are all due to the *atpG* mutations in the three mutants. She also found that in mutants HG203 and HG205 there are identical "GC" deletions in *atpG* that caused truncation of 28 amino acids at the

carboxyl terminal end of the γ subunit of ATP synthsase, while in mutant HG206, there is a "T" deletion in *atpG*, which also caused truncation of 40 amino acids at the C-terminus (Fig. 7). Deletion of either the carboxyl terminus or the amino terminus of the γ subunit causes a failure in the assembly of F_1 (Shin *et al.,* 1992). The C-terminal of γ subunit is important for functioning of F_1 complex as it assembles the catalytic core (F_1). In an *atpG* mutant, F_0 acts only as a proton pore affecting both H^+ flux and intracellular pH. These *atpG* mutants have lower expression of *pckA,* lower growth yield and are Suc^-.

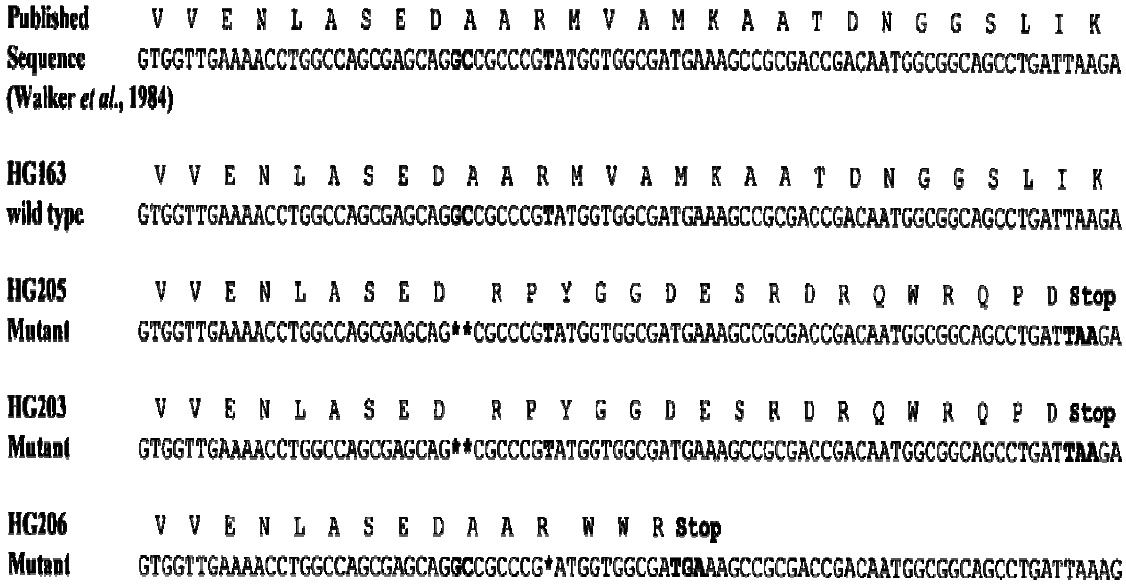

Fig. 7: Published DNA sequence of the C-terminal region of γ subunit of ATP synthase in wild type aligned with sequence of mutants (Madhavan, 2002)

1.6.2. Purpose of this research

After isolating those *atpG* mutants and determining that they had lower Pck activity, it was important to find out how and why the Pck activity was affected. There could be numerous reasons why the Pck activity is low in these *atpG* mutants and for my masters thesis, we decided to investigate whether mutation in *atpG* has some direct effect on *pckA* expression at the transcriptional level. Having a non-functional ATP synthase, we also wanted to find out if electron transport and proton transport are affected in the *atpG* mutants. Therefore, the hypothesis of this study is that mutations in *atpG* do affect Pck expression at the transcriptional level. Moreover**,** *atpG* mutants may have altered proton transport in the cell and this could affect the expression of *pckA* directly or indirectly.

To address these hypotheses, the following objectives were formulated:

1. To repeat growth experiments with *atpG* mutants isolated by Madhavan (2002) and derive accurate doubling time and growth yields.
2. To verify that transcription of *pckA* increases significantly at the onset of stationary phase in *E. coli* and to quantify the steady state mRNA concentrations.
3. To determine whether transcription of *pckA* is affected by *atpG* mutations.
4. To determine rates of proton transport by the electron transport chain in inside-out vesicles of wild type, *atpG* mutants (HG203, HG205 and HG206) and complemented mutants.

CHAPTER TWO

2.0 Materials and Methods:

2.1 Media and Reagents

Growth media such as trytone, agar and yeast extract were purchased from DIFCO Laboratories, Detroit, MI. Minimal Medium A, and Luria-Bertani Broth (LB) (without glucose) were prepared as described by Miller (1972). All Minimal Media (MM) prepared, contained 0.01% vitamin B1 (thiamine) and 0.4% carbon source (glucose, pyruvate or succinate). Antibiotics such as tetracycline (20 μg/ml), chloramphenicol (25 μg/ml), ampicillin (100 μg/ml) and kanamycin (ranged from 5 to 25 μg/ml) were each added as required. Ticarcillin (100 μg/ml) was used in liquid media. PCS scintillation fluid for Pck specific activity assay was bought from Amersham Canada Ltd, Oakville, Ontario. Restriction enzymes were obtained from New England Biolabs inc. (Beverly, MA) and used according to the manufacturer's instruction. Taq polymerase and deoxynucleotide triphosphates were purchased from Amersham Pharmacia Biotech, Inc. (Piscataway, NJ). Most of the biochemical, organic and inorganic chemicals were from Sigma-Aldrich, Canada and all were reagent grade. Kits required for molecular biological techniques were obtained from QIAgen Inc. (Valencia, CA). Custom-designed LUX Fluorogenic primers were ordered online from Invitrogen Canada Inc. (http://www.invitrogen.com). Quantitative PCR kits (Quantitative RT-PCR Thermoscript – one-step system and Superscript™ III Platinum® – two-steps system) were also purchased from Invitrogen Canada Inc.

2.1.1 Bacterial strains and plasmids used in this study

Table 1: Bacterial strains and plasmid used in this study

Bacterial Strains

Strains	Genotype	Phenotype	Reference
HG163	*pps*	Lac^-, Pyr^-	Madhavan S., M.Sc Thesis
HG203	kan^R, *pps*, *atpG551*	Kan^R, Pyr^-, Suc^-, Atp^-, Gro^-, Pck^-	Madhavan S., M.Sc Thesis
HG205	kan^R, *pps*, *atpG552*	Kan^R, Pyr^-, Suc^-, Atp^-, Gro^-, Pck^-	Madhavan S., M.Sc Thesis
HG206	kan^R, *pps*, *atpG553*	Kan^R, Pyr^-, Suc^-, Atp^-, Gro^-, Pck^-	Madhavan S., M.Sc Thesis
HG208	kan^R, *pps*, *atpG551*	Kan^R, Pyr^-, Suc^-, Atp^-, Gro^+, $Pck^\pm$	This work, Gro^+ suppressor of HG203
HG209	kan^R, *pps*, *atpG552*	Kan^R, Pyr^-, Suc^-, Atp^-, Gro^+, $Pck^\pm$	This work, Gro^+ suppressor of HG205
HG210	kan^R, *pps*, *atpG553*	Kan^R, Pyr^-, Suc^-, Atp^-, Gro^+, $Pck^\pm$	This work, Gro^+ suppressor of HG206
MM294A	*pro*, *thi-1*, *endA1*, *hsdR17*, *SupE44*	Pro^-	Backman *et al*. (1976)

Plasmids

Plasmids	Drug resistance	Region expressed	Reference
pACYC184	Cam^R, Tet^R	Vector	Chang and Cohen, (1978)
pDJK35	Cam^R	*atpH,A,G,D,C*	Klionsky and Simoni (1985)
pHG51	Amp^R	*pckA*	Sudom et al. (2003)

2.1.2 Growth of cultures

The OD_{600} nm readings of 5 ml overnight cultures grown in LB medium at 37°C while shaking at 250 rpm were recorded. Volumes of overnight cultures corresponding to OD_{600} nm of 0.001 were inoculated in 500 ml conical flasks containing 200 ml LB and shaken at 250 rpm at 37°C. Samples (10 ml) were kept on ice and used for Pck enzyme assays (5 ml) and RNA extraction (4 ml). OD_{600} nm readings were read on a Pharmacia Biotech Ultrospec 3000 UV-spectrophotometer and growth curves were plotted using Graphpad Prism 4.0 software (GraphPad Software, Inc. San Diego).

2.2 Measuring Pck enzyme activities

2.2.1 CTAB-treated cells

Samples of 5 ml of culture were vortexed with 500 µl of 10X CTAB buffer (0.1% cetyl tetra ammonium bromide or hexadecyl tetra ammonium bromide, CTAB), 3mM $MnCl_2$, 0.2M imidazole, pH 7.5) and centrifuged for 10 min at 2,500 x *g*. The pellets were suspended in 1 ml, 1X CTAB buffer and centrifuged at 16,000 x *g* for two minutes. Supernatants were discarded and the pellet was suspended in 250 µl 1X CTAB buffer. The pellet was immediately vortexed at high speed before placing the tubes on ice for Pck assay.

2.2.2 Pck assay

Pck activities were assayed by measuring ATP-dependent exchange between $NaH^{14}CO_3$ and oxaloacetate (Utter and Kurahashi, 1954). This procedure is a modification of that of Wright and Sanwal (1969). The total volume of the reaction was 500 µl and contained 20 mM oxaloacetate, 20 mM $NaH^{14}CO_3$ (0.55 µCi), 1 mM ATP, 10

mM $MgCl_2$, 0.1 M TRIS-Cl buffer (pH 7.5) and 50 µl of CTAB – treated cells. Oxaloacetate was titrated to pH 7.0 using NaOH. Reactions were started by adding 50 µl of oxaloacetate in a fume hood and stopped after 10 min at 30°C by adding 500 µl of 0.1N H_2SO_4. One drop of octanol was added to each of the vials (to limit foaming) and compressed air was bubbled vigorously for 10 min to remove $^{14}CO_2$. The vials were counted with 3.5 ml PCS scintillation fluid. HG163 was used as the wild type control. Protein was assayed using the Lowry method (Geiger and Bessman, 1972) with 1 mg/ml BSA as a standard. This procedure was adapted from Lowry *et al.* (1951).

2.3 ATP synthase enzyme activity

2.3.1 Preparation of inside out vesicles

Inside out vesicles of wild type and mutant strains were prepared by inoculating 20 ml of overnight culture into two litres of Minimal Media A containing 0.3% glucose and 0.25% casamino acids. Flasks were incubated at 37°C while shaking overnight at 250 rpm. Cultures were centrifuged at 2,700 x *g* for 15 minutes at 4°C. Pellets were suspended in cold 50 mM Tris (pH 7.8) containing 5 mM $MgSO_4$, centrifuged again, and resuspended in cold buffer. The pellets were washed twice with cold 0.8% NaCl before centrifuging at 2,700 x *g* for 15 minutes at 4°C. Pellets collected were resuspended in ice-cold Tris-Mg EDTA buffer (50mM Tris and 5mM $MgSO_4$, containing 1 mM EDTA). For every 1 gram of pelleted cells, 10 ml of cold Tris-Mg EDTA buffer was added. The cells were passed through a French Press at 10,000 psi and centrifuged at 11,000 x *g* for 15 minutes at 4°C. Supernatants were collected and centrifuged at 17,640 x *g* for 1 hour at 4°C in a 60Ti rotor using a Beckman ultracentrifuge. Each pellet was resuspended in 2

ml ice-cold Tris-Mg EDTA buffer, homogenised with a hand held glass (JENCONS model) homogeniser before storing at -70^{o}C.

2.3.2 ATP synthase assays

The ATP synthase reaction was measured by hydrolysis of ATP to yield inorganic phosphate (Pi) and ADP. Pi was then measured by the reaction with ammonium molybdate to produce ammonium phosphomolybdate. Phosphomolybdate complexes were measured by converting them to molybdenum using ANSA reagent (1-amino-2 naphthol-4 sulfonic acid containing sodium bisulfite and sodium sulfite) (Fiske and Sunnarow, 1925).

Phosphate free or acid washed tubes were used for the reactions. Three sets of reactions were carried out: with Mg^{2+}; without Mg^{2+} (control) and with Mg^{2+} plus ATP synthase inhibitor, DCCD (1,3-dicyclohexylcarbodiimide). Reaction tubes contained 0.78 ml 50 mM TRIS-sulphate buffer, pH 7.8 containing 1mM EDTA, 75 µl 0.04 M $MgCl_2$ and 0.1 ml membranes (1: 100 dilution). Tubes were incubated at 37^{o}C for 5 min. The reactions were started with 50 µl of 0.1 M ATP and incubated for 10 min. The reactions were stopped after 10 min with 1 ml of 10% TCA (Trichloroacetic acid) and placed on ice. To control tubes, TCA was added before ATP and DCCD (stocks were 10 mM in methanol). A control experiment with 10 µl methanol instead of DCCD was also carried out. The tubes were centrifuged at 13,000 x *g* for 10 min in a Beckman high-speed centrifuge model J2-21.

The amount of Pi generated in each experimental tube was interpolated from a standard graph of A_{660} against Pi. Protein concentration (mg/ml) of the membranes was

determined by Lowry assay and specific activity of ATPase in membranes was calculated in μmoles·min^{-1}·mg^{-1}.

2.4 Reverse transcriptase real time polymerase chain reaction (RT-rtPCR) to measure mRNA expression during bacterial cell growth.

2.4.1 RNA extraction

Samples of 1 ml were collected from *Escherichia coli* cultures. Throughout this study, different methods of RNA extractions were used. First, we used two kits: (1) RNAqueous (small-scale Phenol-Free total RNA isolation kit) and (2) RiboPure Bacteria (kit specifically design for RNA extraction in prokaryotes, which uses Zirconia Beads to disrupt cell structure) from Ambion Inc. (www.ambion.com). The second kit was a newly developed RNA extraction kit from Ambion. However, the quantity and quality of RNA extracted from both kits were extremely poor, so we used an RNA extraction method developed by Dr. George Mackie (1989) as described in appendix I.

2.4.2 RNA quality and quantity determination

The purity and integrity of RNA extracted was calculated using the ratio of absorbance read at 260nm and 280nm (A_{260}:A_{280} ratio). Five μl of RNA was dissolved in 995 μl DEPC water. Good RNA quality is observed when A_{260}:A_{280} ratio lies between 1.8-2.1 (http://core.img.cas.cz). Five μl of RNA extracted was also run on a 1% denaturating agarose gel (containing MOPS [3-(N-morpholino) propanesulfonic acid] and formaldehyde) to determine its integrity. Concentration of RNA (μg/ml) was calculated using the A_{260nm}. RNA (1μg) of mutants and wild type were each treated with

RNase-free DNAase enzyme (1 unit) (From Invitrogen inc.) to digest any bacterial DNA present in the RNA sample.

2.4.3 cDNA synthesis

Complementary DNA (cDNA) was synthesised using Superscript™ III Platinum® two-Step quantitative RT-PCR kit (Invitrogen). The two-Step system involved (i) the synthesis of cDNA (ii) quantitative PCR performed in another tube. Reverse transcriptase (RT) enzyme mix contained Superscript™ III reverse transcriptase and RNaseOUT™ Recombinant ribonuclease inhibitor. The RT enzyme has been engineered to reduce RNase H activity as well as to increase its thermal stability (Kotewicz M *et al.,* 1985). It is also not inhibited by ribosomal and transfer RNA, thus allowing synthesis of cDNA from total RNA. RNaseOUT is an RNase inhibitor protein that protects the RNA from being degradaded from ribonuclease contamination. The optimised RT buffer for cDNA synthesis contains random RNA hexamers, 10 mM $MgCl_2$ and dNTPs. For cDNA synthesis, to tubes containing 0.386 ug of DNAase-treated RNA, 5 µl RT buffer and 0.75 µl RT enzyme mix were added. The tubes were gently mixed before being incubated in a Perkin Elmer PCR machine (cDNA synthesis program: 25^{o}C for 10 min., 48^{o}C for 50 min and 85^{o}C for 5 min). The tubes were chilled on ice before adding 0.5 µl RNase H to each tube followed by incubation for 20 min at 37^{o} C. Complementary DNA was then stored at -20^{o} C. RNase H was added to remove the RNA template from cDNA:RNA hyrid molecules after first-strand synthesis to increase quantitative PCR sensitivity.

2.4.4 Lux primers

Custom-designed LUX fluorogenic primers (Invitrogen) were used for quantitative PCR. LUX (or **L**ight **U**pon e**X**tension) primers consist of a pair of primers consisting of a forward fluorogenic primer with a fluorophore attached to its 3' end, as well as an unlabeled reverse primer. The fluorogenic primer has a short sequence tail of 4 - 6 nucleotides on the 5' end that is complimentary to the 3' end of the primer. The resulting hairpin secondary structure (Fig. 8) provides optimal quenching of the fluorophore.

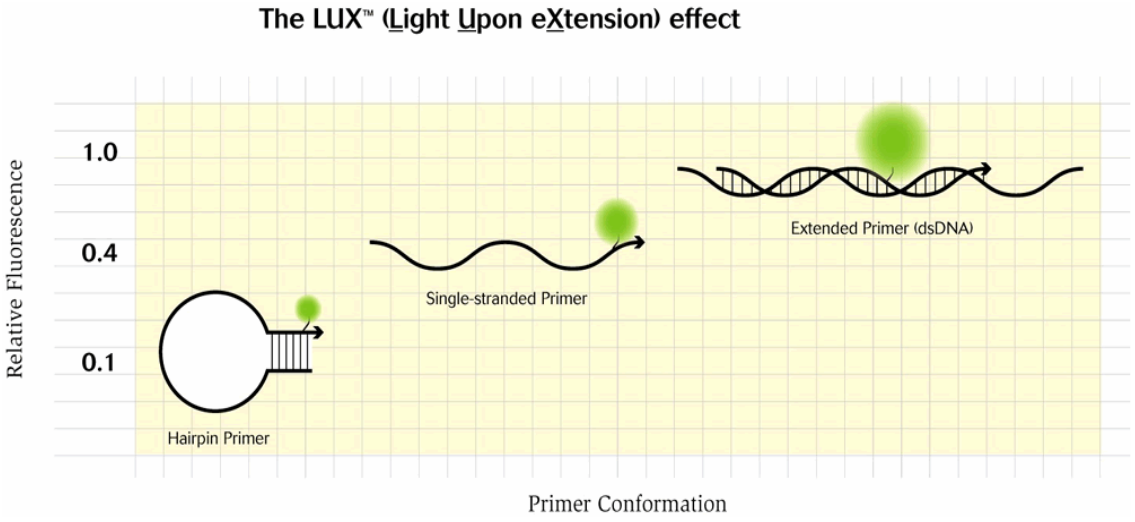

Fig. 8: Quenching of the fluorophore (represented as green circle) of the LUX forward primer. When released from the hairpin form and incorporated into the double-stranded PCR product, there is dequenching of fluorophore that causes an increase of relative fluorescence of up to 10-fold. This figure was taken from Invitrogen web site: (http://www.invitrogen.com/content.cfm?pageid=3978#HowLuxWorks)

When the primer is incorporated into the double-stranded PCR product, quenching of the fluorophore decreases and the fluorescence intensity increases by up to 10-fold. The fluorogenic LUX primer is labelled with FAM (6-carboxy-fluorescein) dye (Fig. 8). It has excitation/emission wavelengths of 490/520nm. In this study, we used oHG177 (CGCGGTAAATCTATGAGCGTTGTCGG), a 27 base primer homologous to

the 5' region of *pckA*, that was labelled by FAM and oHG178 (CGCATTTCACTGCTCCTTAGCC), a 22 base unlabelled primer for the *pckA* gene. The PCR product generated using those two primers was 93 base pairs long.

2.4.5 Quantitative PCR

For quantitative PCR, DNA Engine Opticon® 2 Real-time PCR Detection system (by MJ research/Biorad research) was used. Initially we started with a one-step system RT-PCR kit called Platinum ® Quantitative RT-PCR Thermoscript from Invitrogen. This kit consists of a high temperature reverse transcriptase (avian, ribonuclease H deficient provides highly specific and efficient cDNA synthesis at elevated temperatures) and an automatic hot-start Platinum® *Taq* DNA polymerase. The one-step system allows for both the generation of cDNA and subsequent amplification of the cDNA in one tube. During cDNA synthesis, a mixture of monoclonal antibodies inhibits *Taq* activity. When cDNA synthesis is completed, reverse transcriptase enzyme is denatured during the "denaturation" step of PCR thus restoring full function of *Taq* activity. The two-step method consists of Invitrogen's Superscript™ III Platinum® two-Step quantitative RT-PCR kit. This kit consist of Superscript™ III reverse transcriptase enzyme which provides highly specific and efficient cDNA synthesis at elevated temperatures as well as an automatic hot-start Platinum® *Taq* DNA polymerase with integrated UDG (uracil DNA glycosylase) carry over prevention technology. UDG and dUTP in the buffer prevent reamplification of carry-over PCR product between reactions. The presence of dUTP ensures that any amplified DNA will contain uracil while UDG removes uracil residues from single or double stranded DNA, thus preventing dU-containing DNA from serving as template in future PCRs. The *Taq* DNA polymerase (60 U/ml) buffer

consisted of 40 mM Tris-HCl (pH 8.4), 100mM KCl, 6mM $MgCl_2$, 400 μM dGTP, 400 μM dATP, 400 μM dCTP, 800 μM dUTP, 40 U/ml UDG, and stabilizers. For the quantitative PCR reactions, low profile tubes (recommended for DNA Engine Opticon® 2 Real-time PCR Detection system from Biorad) were used. In each tube 0.25 μg cDNA was added followed by 12 μl *Taq* buffer, 0.3 μl of 10 mM oHG177, 0.3 μl of 10 mM oHG178 and the volume was made up to 25 μl by the addition of water. The tubes were well mixed, centrifuged lightly and placed on the 96 well rack of the DNA Engine Opticon® 2 Real-time PCR Detection system. Each sample was run in triplicate. Conditions used for the setting of quantitative PCR resulted from the modification of the Ambion® protocol where the qPCR step and cycle have been optimized as shown in Appendix 2.

2.4.6 Normalising real-time RT-PCR data

The question of how to analyse quantitative real time RT-PCR data has still not been answered to universal satisfaction. Several methods (Bustin A, 2005) have been generated for normalising real time RT-PCR data, among which two methods were used in this study. The first method known as the relative (or comparative threshold [C_t]) method) is used to compare the changes in steady-state mRNA levels of the target gene with one or several endogenous reference genes. This method is considered a simple and most popular method for internally controlling for error in real time RT-PCR for eukaryotic mRNAs. The second method used in this study is the standard curve method (or absolute method). This method compares expression of mRNA levels to an external standard.

2.4.6.1 Relative method

The comparative C_t method involves normalising the C_t values of the gene of interest to an appropriate endogenous housekeeping gene. The amplification efficiencies of the target and the endogenous reference must be approximately equal for the relative method to be valid. It is based on the expression levels of a target gene versus a housekeeping gene. To calculate the expression of a target gene in relation to an adequate reference gene various mathematical models are established (Bustin, 2004) and the model that I started using for quantification was derived from the paper published by Livak *et al*. (2001). The equation is as followed:

Fold change in gene expression

$$= 2^{-\Delta\Delta C_t}$$

$$= 2^{-[(C_t\, pckA_{\text{time x}} - C_t\, 16sRNA_{\text{time x}}) - (C_t\, pckA_{\text{time 0}} - C_t\, 16sRNA_{\text{time 0}})]}$$

The cycle threshold (C_t) is the first cycle in which there is a significant increase in fluorescence above the background or a specified threshold and it is determined from the primary curve. The smaller the C_t value, the larger the amount of specific mRNA is present. In my experiment, there is no RNA extracted at time zero as RNA level extracted at that time is too low. The earliest time for RNA extraction is 1 hour and that time is considered as (time 0) in the equation. Once the fold change expression is obtained for each sample, mean fold change in gene expression versus time was plotted. However, when this method was tried using *pckA* as the target gene and *rrn* (16srRNA*)* as the housekeeping gene, the amplification efficiencies were not constant and varied between the different time points as well as between the strains, leading to unreliable results. If the expression of the housekeeping gene is variable, then the noise of the assay

is increased leading to difficulty in detecting changes in mRNA expression of the target gene (Dheba *et al.,* 2006).

2.4.6.2 Absolute method

For the absolute method, a standard curve was generated using the plasmid pHG51. pHG51 plasmid contains the *pckA* gene and consists of 4750 base pairs. A series of three serial dilutions (10-fold) ranging from 30.4 nmol to 30.4 pmol were prepared. Each serial dilution (2.5 µl) was added to low profile tubes containing 12 µl *Taq* buffer, 0.3 µl of 10 mM oHG177, 0.3 µl of 10 mM oHG178 and the volume was made up to 25 µl with water. For each serial dilution, triplicate tubes were prepared. The tubes were well mixed, centrifuged lightly and placed on the 96 well rack of the DNA Engine Opticon® 2 Real-time PCR Detection system along with sample tubes. Conditions used for quantitative PCR resulted from the modification of the Ambion® protocol where the qPCR step and cycle have been optimised as shown in Appendix 2. A plot of C_t vs. the logarithm of concentration resulted in a straight line, the standard curve, fitted by linear regression. Each time quantitative PCR was performed on samples, a standard curve was generated and data were normalised using the corresponding standard curve. Positive controls (corresponding to the addition of known concentrations of plasmid) were also added to the quantitative PCR to determine the efficiency of qPCR as well as to validate the standard curve results. PCR products were run on 1% agarose gels to check integrity of the qPCR product.

2.5 Molecular biology methods

2.5.1 PCR amplification

Mutant as well as wild type chromosomal DNA were amplified using oHG177 and oHG178 primers specific to *pckA*. The expected size of the fragment was 93 bp. The PCR mixture consisted of 10 µl of 10X PCR buffer (100 mM Tris-HCl, pH 9.0, 15 mM $MgCl_2$ and 500 mM KCl) (Amersham. Inc), 8 µl of 2.5 mM deoxynucleotides, 15 ng of DNA, 50 pmoles of primers, 1µl of Taq polymerase (5000 units/ml) and sterile water to a total volume of 100 µl. The PCR incubation cycle was as follows: denaturation at 94^{o}C for 1 min, annealing at 55^{o}C for 1 min and extension reaction at 72^{o}C for 1 min. The cycle was repeated 35 times, followed by 72^{o}C for 5 min and held at 4^{o}C.

2.5.2 DNA electrophoresis

2.5.2.1 Agarose gel Electrophoresis – 1%

DNA samples (30 µl) mixed with 4 µl agarose loading buffer (36% urea, 0.5% bromophenol blue, 0.5% xylene cyanol green) were loaded on a 1% agarose gel containing 0.1 µg/ml ethidium bromide and then electrophoresed. The 100 bp DNA ladder and the 50 bp DNA ladder (1.0 µg/ml) from Invitrogen Inc. were used as DNA moleculer weight standards. DNA fragments were separated at a constant voltage of 75 V in 1x TBE (0.09 M Tris, 0.5 mM EDTA (pH 8.0), 0.09 M H_3BO_3) buffer, pH 8.3, containing 0.1 µg/ml of ethidium bromide. DNA fragments were visualized with a UV transilluminator with 310 nm ultraviolet light and photographed using Polaroid type 55 film (Polaroid Corporation, Cambridge, MA) and a Kodak Wratten No. 2 filter.

2.5.2.2 Denaturating Agarose Gel Electrophoresis

Denaturating Agarose gels were prepared using 1% agarose, 10 ml of 10X MOPS running buffer (400 mM MOPS, pH 7.0, 100 mM sodium acetate and 10 mM EDTA) and 18 ml of 12.3 M formaldehyde (Ambion RiboPure^{TM}-Bacteria instruction manual) . One µg of each RNA sample (containing 5 µl 10X MOPS running buffer, 9 µl of 12.3 M formaldehyde and 25 µl formamide) was heated at 55^{o}C for 15 min in 1X MOPS running buffer. Loading dye (Sigma-Aldrich) containing 0.5 µg/ml ethidium bromide and 10 µl formaldehyde was added to the RNA samples. The samples were loaded and allowed to electrophorese at 5 V/cm until the bromophenol blue (fast-migrating dye) has migrated one-half to two-thirds of the length of the gel. The gel was visualised using a UV transilluminator with 310 nm ultraviolet light and photographed using Polaroid type 55 film and a Kodak No. 2 filter.

2.5.2.3 SDS acrylamide gel electrophoresis

Protein samples were run in 10% acrylamide SDS gels as described by Laemmli, (1970).

2.5.3 Plasmid DNA purification

ER2429 cells contained pACYC184 plasmid (Tet^{R}) while MM294 cells contained pDJK35 (*atpG*$^{+}$, Cam^{R}) plasmid. One colony from each strain was inoculated into tubes containing 5 ml LB containing selective antibiotic. Tetracycline (20 µg/ml) or chloramphenicol (25 µg/ml) was added and cells were allowed to grow approximately 8 hours at 37^{o}C while shaking at *ca.* 250 rpm. Each culture (250 µl) was inoculated into two conical flasks containing 250 ml LB with selective antibiotic and incubated

overnight at 37°C while shaking vigorously. The cells were harvested by centrifuging at 2,500 x *g* for 5 min at 4°C and the pellet was used for plasmid isolation as per QIAfilter Plasmid Maxi protocol (QIAgen Plasmid Purification Handbook, 1999) (www1.qiagen.com/HB/plasmid purification).

2.5.4 Electroporation

2.5.4.1 Preparation of competent cells for electroporation

Chemical transformation was found to be unsuccessful for transfer of plasmids to the *atpG* mutants (Madhavan, 2002 and this work); therefore, electroporation was used. One liter of LB was inoculated with 1% overnight inoculum and grown to mid-log phase with shaking at 37°C. The different bacterial strains used in this study as competent cells for electroporation were prepared as described by Madhavan (2002). The culture was centrifuged at 2,500 x *g* for 15 min and the pellet was resuspended gently in 1 liter of ice-cold 10% glycerol. The cells were centrifuged again for 5 min at 5000 rpm. The pellet thus obtained was washed four times in 10% glycerol and each time the volume of glycerol was reduced by half. The last pellet was resuspended in 4 ml of 10% glycerol. Aliquots of competent cells (40 µl) were dispensed into cold sterile microfuge tubes, frozen immediately in a -70°C methanol bath and stored at -70°C.

2.5.4.2 Electroporation and plating

Competent cells were allowed to thaw gently on ice. 2 µl of the appropriate plasmid was added to the 40 µl of competent cells and kept on ice for 1 min. The mixture was transferred into a chilled sterile electroporation cuvette (Bio-rad laboratoried, Inc. Hercules, CA), and the cells were exposed to a voltage pulse of 1.8 kV

using the *E.coli* Pulser (Bio-rad laboratories, Inc. Hercules, CA). After electroporation, 1 ml of SOC medium (American Biorganics, Inc. Niagara falls, NY) was immediately added to the cuvette and mixed well by pipeting several times up and down the cuvette. The cells in SOC solution were then transferred into sterile 1.5 ml microfuge tubes and placed on a shaker at 37^{o}C for one hour. Following the incubation, the tubes were centrifuged at 11,000 x *g* in an Eppendorf 5415D centrifuge and the pellet obtained was suspended in 100 µl SOC, plated on appropriate antibiotic containing plates and incubated at 37^{o}C for 24 h.

2.6 Detecting formation of the electrochemical H^+ gradient.

2.6.1 Fluorescence quenching

Fluorescence quenching of acridine orange was used to measure H^+ flux in inside-out vesicles of wild type (HG163), mutants (HG203, HG 205, HG206) and strains with vector plasmid pACYC184 or *atpG*$^+$ plasmid pDJK35. Inside-out vesicles of these bacterial strains were made as described in Section *2.3.1* and protein concentrations were measured by the Lowry method (Lowry *et al.* (1951). Volumes of membranes corresponding to 300 µg of protein were suspended in 3 ml of 10 mM Tricine choline buffer (pH 8.0) that contained 140 mM KCl, 5 mM $MgCl_2$, 1 µg/ml valinomycin and 1 µM acridine orange (Sigma-Aldrich). Tricine choline stock (100 mM) was made by dissolving tricine in 50 ml double deionised water and pH was adjusted to 8.0 using 50% w/w choline base. Valinomycin (100 µg/ml) was prepared in 99% ethanol. Acridine orange (37 µg/ml) was freshly prepared in double deionised water. Acridine orange

penetrates the membrane vesicles and emits fluorescence at 530 nm with an excitation of 490 nm. Once protonated, acridine orange no longer emits fluorescence.

2.6.2 Fluorescence measurements

In a cuvette with stirrer, 3 ml of 10 mM tricine choline buffer was added followed by bacterial inside out vesicles (300 μg of membrane protein). Valinomycin (100 μg/ml) and acridine orange (100 μM) were also added to the cuvette. The cuvette was placed in the Hitachi F-2500 FL spectrophotometer and allowed to stabilise for 41 seconds before 4 μl of 0.25 M ATP was added and the experiment was allowed to run up to 120 sec. Blank samples contained all the reagents as in the sample cuvette except membrane protein. The software used to set the Hitachi F-2500 FL spectrophotometer was "FL Solution". Time courses of quenching were recorded with excitation at 490 nm and emission at 530 nm. The excitation and emission slits were both set at 5.0 nm. Response time was 0.08 sec.

2.6.3 Generation of data

The data from the Hitachi F-2500 FL spectrophotometer (in excel format) were transferred to Graph Prism 4.0 software where curves were fitted using non-linear regression.

CHAPTER THREE

3.0 Results

3.1 Growth and phenotypes of *atpG* mutants and wild type HG163

3.1.1 Phenotypse of atpG mutants and wild type HG163

The phenotypes of the bacterial strains used in this study were verified every time a growth curve experiment was performed. Bacterial strains were plated on minimal medium A (MM) containing glucose, succinate or pyruvate respectively. The data obtained are shown in Table 2 below. Wild type strain HG163 (*pps*$^{-}$) grew on MM plates containing either glucose or succinate as sole carbon sources but did not grow on MM plates that contained pyruvate only. The *atpG* mutant strains grew on MM plates that contained glucose only but not on MM plates that contained succinate or pyruvate as sole carbon sources.

All bacterial strains were also plated on antibiotic plates containing kanamycin. As expected, the wild type strain HG163 did not grow on kanamycin plates while *atpG* strains did grow on them (Thorbjarnadottir *et al.,* 1978). HG203, HG205 and HG206 grew faster on kanamycin plates compared to HG208, HG209 and HG210.

Table 2: Growth of wild type (HG 163) and *atpG* mutants (HG203, HG205, HG206, HG208, HG209 and HG210) on minimal media A (MM) containing glucose(G), succinate(S), pyruvate(P) and LB with kanamycin (25ug/ml).

Bacterial strains	phenotype	MM + G plate	MM+S plate	MM+P plate	K plate
HG163	-	+	+	-	-
HG203	Gro^-	+	-	-	+
HG205	Gro^-	+	-	-	+
HG206	Gro^-	+	-	-	+
HG208	Gro^+	+	-	-	+
HG209	Gro^+	+	-	-	+
HG210	Gro^+	+	-	-	+

3.1.2 Growth of atpG mutants and wild type HG163

Growth curves for LB medium were generated as described in Materials and Methods (See section 2.1.3). Briefly, culture flasks containing LB medium were inoculated at an OD_{600nm} of 0.001 with bacterial strains (HG163, HG203, HG205 and HG206). Growths of *atpG* mutants and wild type HG163 were monitored up to 18 hours and Log OD_{600nm} was plotted as a function of time as shown in Figure 9.

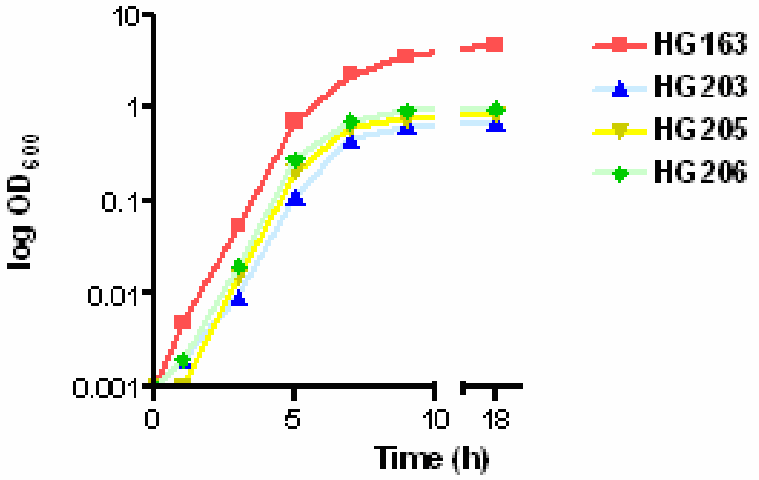

Fig. 9: Growth curves of *atpG* mutants (HG203, HG205, HG206) and wild type HG163. Growth was monitored from 0 hours up to 18 hours after inoculation in LB. The experiments were repeated several times and the figure shows representative data.

The results showed that wild type HG163 grew at a faster rate during lag and log phase (Table 3) as compared to all *atpG* mutants (HG203, HG205, HG206). Further, HG163 had a higher growth yield in stationary phase and the OD_{600nm} was higher that the *atpG* mutants. It was also observed that HG203 grows slower than HG205 and HG206 during both phases (Fig. 9 and Table 3). However, the growth yield in stationary phase was similar for all three mutants. Therefore, it seems that the *atpG* mutations have effects on the growth of the bacteria.

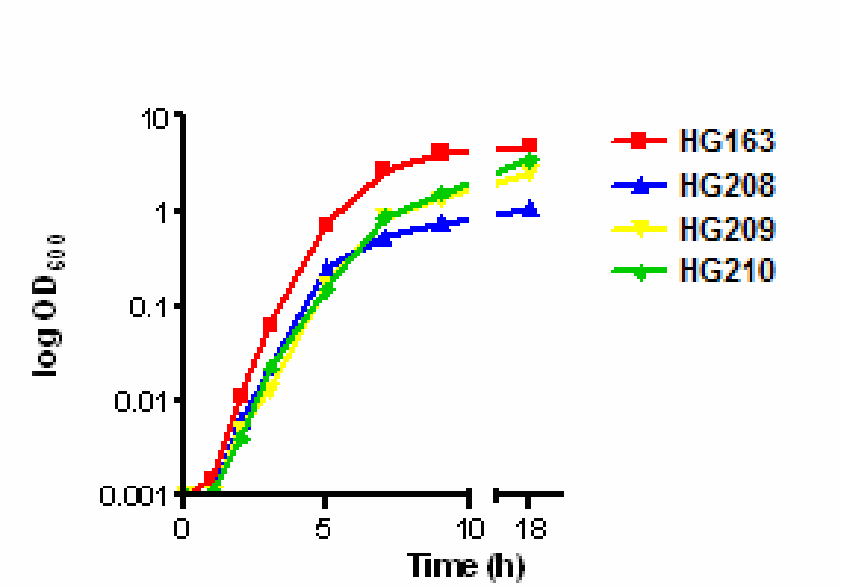

Fig. 10: Growth curve of *atpG* mutants (HG208, HG209 and HG210) and wild type HG163 as a function of time. Growths were monitored from 0 hours up to 18 hours after inoculation in LB. The experiments were repeated several times and the figure shows representative data.

Strains HG208, HG209 and HG210 were spontaneous Gro^+ isolates of Gro^- strains HG203, HG205 and HG206, respectively, which had larger colonies. Growth curves for strains HG208, HG209, HG210 and wild type HG163 were generated. As shown before, wild type HG163 grew at a faster rate during log phase as compared to all *atpG* mutants (HG208, HG209, HG210) (Fig. 10 and Table 3). However, HG209 and HG210 growth yields in stationary phase were higher than HG205 and HG206 and closer to wild type HG163. In addition, it was also observed that HG208 growth yield in stationary phase was lower than that of HG209, HG210 and HG163 (Fig. 10) and Table 3. Therefore, it seems that *atpG* mutants HG209 and HG210 were different from *atpG* mutants HG205 and HG206.

The doubling times have been calculated for all the *atpG* strains and for the wild type strain. The percentage growth yields related to the wild type strain (HG163) were also determined. These data are presented in Table 3. The results demonstrated that the

maximum growth yield reached for HG163 in LB was an OD_{600nm} of 4.75 while for *atpG* mutants maximum growth yield ranged between 0.70 – 3.45 (Table 3).

Table 3: Doubling time (in min), growth yield (OD600) and percentage growth yield of *atpG* mutants and wild type HG163.

Bacterial strain	TD (min)	Max Growth yield (OD600nm)	% growth yield (related to wild type)
HG163	25	4.75 ± 0.23 *	100
HG203	34	0.70 ± 0.082	15
HG205	32	0.88 ± 0.059	18
HG206	30	0.99 ± 0.008	21
HG208	31	1.0 ± 0.082	21
HG209	34	2.5 ± 0.24 *	53
HG210	34	3.45 ± 0.35 *	73

* OD's greater than 1.0 were determined by diluting cultures 1/10 in LB medium

HG203, HG205 and HG206 grew to lower growth yields (Table 3) compared to HG208, HG209 and HG210 even, though the doubling times were not significantly different. HG208, HG209 and HG210 had growth yields ranging from 21% to 73% of wild type while HG203, HG205 and HG206 had growth yield ranging from 15% to 21% of wild type (Table 3). This indicated that the Gro^+ derivatives (HG208, HG209 and HG210) had larger colonies than the original *atpG* mutants (HG203, HG205 and HG206), due to increased growth yields, that were still not as high as for wild type.

3.2 Pck enzyme activities in *atpG* mutants and wild type HG163

Pck specific activities of *atpG* mutants (HG203, HG205, HG206) and wild type (HG163) were measured using ATP-dependent exchange of ^{14}C between $NaH^{14}CO_3$ and oxaloacetate as described in Materials and Methods (section 2.3.2). The Pck enzyme specific activities were monitored for nine hours following incubation of LB media with their respective 0.001 OD_{600nm} bacterial strain. The results are shown in the graph below.

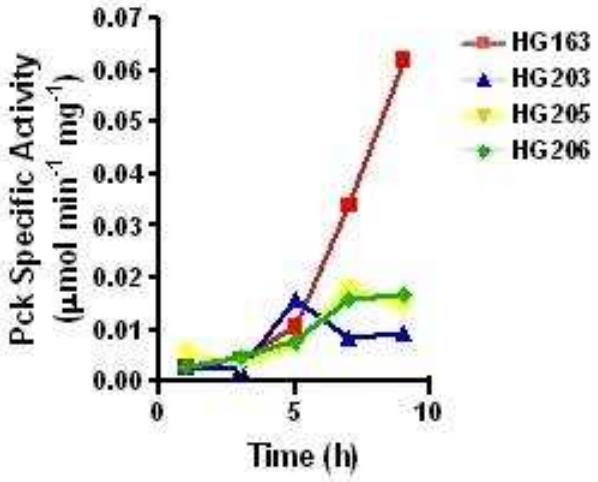

Fig. 11: Pck enzyme Specific Activity ($\mu mol \cdot min^{-1} \cdot mg^{-1}$) in *atpG* mutants and wild type, HG163. Pck Specific Activity was measured as a function of time starting from 0 hours to 9 hours.

The results showed that in wild type, Pck enzyme activity started to increase by 5 hours after inoculation, which corresponded to the onset of early stationary phase as indicated by growth curve in Fig. 11. By nine hours, Pck enzyme specific activity in wild type reached a maximum of 0.062 ± 0.0005 $\mu mol \cdot min^{-1} \cdot mg^{-1}$. Previous experiments have shown that Pck specific activities reached a peak at 8 to 9 hours on this medium and declined slightly thereafter (Madhavan, 2002). For the *atpG* mutants, as in wild

type, at the onset of stationary phase (which corresponded to 5 hours on growth curve), there was an induction in Pck enzyme specific activity. However, the Pck specific activities of HG203, HG205 and HG206 were significantly lower compared to HG163. HG203 has a maximum Pck Specific activity occurring at 5 hours (0.0160 ± 0.0003 $\mu mol \cdot min^{-1} \cdot mg^{-1}$). HG205 and HG206 Pck Specific activities reached a maximum by 7 and 9 hours (0.0165 ± 0.0021 $\mu mol \cdot min^{-1} \cdot mg^{-1}$ and 0.0155 ± 0.0021 $\mu mol \cdot min^{-1} \cdot mg^{-1}$) (Fig. 11). These results suggest that mutation in *atpG* affects the Pck levels and that *atpG* may be a factor in the induction during stationary phase.

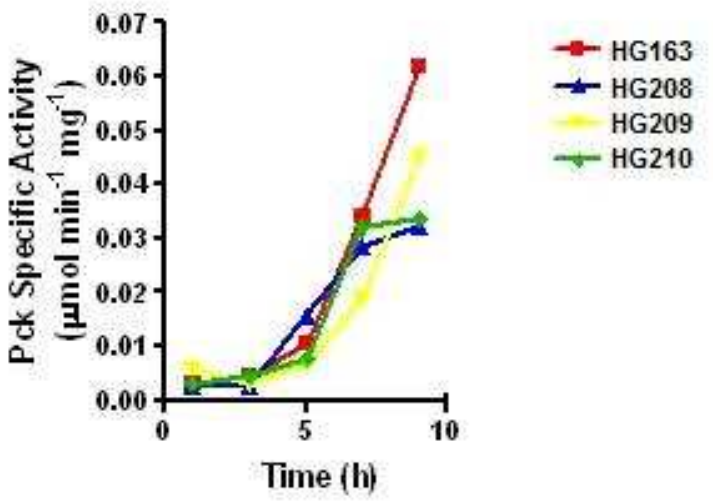

Fig. 12: Pck enzyme specific activity ($\mu mol \cdot min^{-1} \cdot mg^{-1}$) in *atpG* mutants and wild type, HG163. Pck Specific Activity was measured as a function of time starting from 0 hours to 9 hours.

Pck specific activities of Gro^+ suppressors of *atpG* mutants (HG208, HG209, HG210) were significantly higher as compared to HG203, HG205 and HG206; although, lower than for wild type, HG163. HG208 and HG210 had maximum Pck Specific Activities of 0.0315 ± 0.0007 $\mu mol \cdot min^{-1} \cdot mg^{-1}$, while HG209 had Pck Specific Activity

of 0.0450 ± 0.0005 µmol·min^{-1}·mg^{-1} (Fig. 12). The average Pck enzyme specific activities of HG203, HG205 and HG206 were approximately 21% compared to wild type HG163 (Fig.12). However, HG208 and HG210 had Pck specific activities around 51% of wild type Pck specific activity and HG209 was around 73% of wild type, HG163 (Fig. 12). Thus, the Pck enzyme activity in the Gro^{+} suppressors (HG208, HG209, HG210) was for some unknown reason being partially restored compared to the original *atpG* mutants, HG203, HG205 and HG206.

3.3 ATP synthase Specific Activity

ATP synthase specific activities in wild type HG163, *atpG* mutants and Gro^{+} suppressors were determined. This was important as the Gro^{+} suppressors (HG208, HG209 and HG210) had higher levels of Pck enzyme specific activity compared to the original Gro^{-} *atpG* mutants (HG203, HG205 and HG206). ATP synthase specific activities in wild type and *atpG* mutants are summarised in the graphs below (Fig. 13 A-B). For the wild type HG163, the results were as expected with a high ATP synthase specific activity as shown by Fig. 13. The average ATP synthase specific activity in wild type was 0.23 ± 0.035 µmol·mg^{-1} protein. For HG203, HG205 and HG206, the level of ATP synthase specific activity was the lowest. HG203 had a specific activity of 0.0067 ± 0.0012 µmol·mg^{-1}. HG205 had a specific activity of 0.0077 ± 0.0057 µmol·mg^{-1} while HG206 had a specific activity of 0.006 ± 0 µmol.mg^{-1} (Fig. 13A).

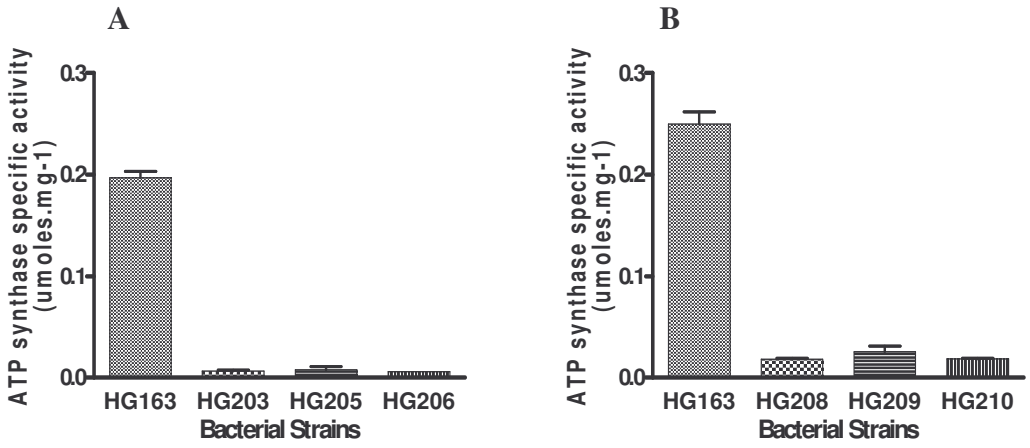

Fig. 13 A-B: ATP synthase Specific Activity in wild type (HG163) and *atpG* mutants. Error bars correspond to standard errors of the means.

From the graph in Fig. 13B, ATP synthase activity of Gro^+ suppressors, HG208, HG209 and HG210 was higher than for the original *atpG* mutants, HG203, HG205 and HG206. HG208 had a specific activity of 0.018 ± 0.0017 $\mu mol \cdot mg^{-1}$ and HG209 had a specific activity of 0.025 ± 0.0098 $\mu mol \cdot mg^{-1}$ while HG210 had a specific activity of 0.019 ± 0.0006 $\mu mol \cdot mg^{-1}$ (Fig. 13B). Thus, ATP synthase specific activity in Gro^- *atpG* mutants ranged from 0.006 to 0.007 $\mu mol \cdot mg^{-1}$, while Gro^+ suppressors ranged from 0.018 to 0.025 $\mu mol \cdot mg^{-1}$. These results indicate that Gro^+ suppressors still have significant defects in ATP synthase activity since wild type ATP synthase activity was 10 fold higher.

3.4 Real Time Reverse transcriptase PCR assay of *pckA* mRNA levels

Since we found that *atpG* mutants have lower Pck activities, lower growth rates and yields, using real time RT-PCR, we assessed whether *pckA* is affected by *atpG* mutations at the transcriptional level using those Gro^- *atpG* mutants (HG203, HG205, HG206) and Gro^+ *atpG* mutants that had their Pck enzyme activity slightly reverted (HG208, HG209 and HG210).

3.4.1 RNA quality

Samples were taken from bacterial cultures every 2 hours after the 1st hour of growth. One ml of bacterial culture was taken from each flask for RNA extraction procedure (See section *2.4.1*). Extraction of RNA used the method of Mackie (1989, Appendix 1). The quality of RNA extracted was determined by two methods. The first method was to use OD values read at 260nm and 280nm (A_{260}:A_{280} ratio). Good RNA quality is observed when the A_{260}:A_{280} ratio lies near 2.0 and a range between 1.8 – 2.1 is considered acceptable (http://core.img.cas.cz). All of the RNA extracted had ratios in the range of 1.85 – 2.0. The second method was to electrophorese the RNA extracted on 1% denaturating agarose gel (containing MOPS and formaldehyde as described in methods section 2.5.2.2). One of the denaturating agarose gels is depicted below (Fig. 14). RNA samples were extracted from HG163, HG203, HG205 and HG206.

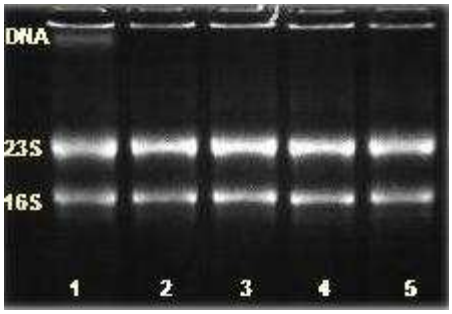

Fig. 14: Total RNA isolated (1µg) was separated on a 1% denaturating agarose gel in formaldehyde/MOPS buffer. In all the RNA samples loaded on this gel, 16S and 23S ribosomal RNA (rRNA) are seen clearly. First lane consists of RNA extracted from HG163. Beside the 2 rRNA bands, there is also a band of high molecular weight in lane 1 that corresponds to some bacterial DNA in lane 1. Lanes 2-5 consist of RNA samples treated with RNAse free DNAse. Lane 2: HG163, Lane 3: HG203, Lane 4: HG205, lane 5: HG206.

In all of the RNA samples loaded on this gel, two ribosomal RNA bands were highly visible. They were the 16S ribosomal RNA (labelled 16S on the gel) and the 23S ribosomal RNA (labelled 23S) (Fig. 14). The size of the 16S RNA was approximately 1.4 kbp (usually size of 16S RNA is 1.5 kbp) while that of the 23S RNA was around 2.8 kbp (usually the size is around 3.0 kbp). From a denaturating agarose gel, the quality and integrity of extracted RNA can be determined by the quality of the bands and the intensity of the 16S band related to the 23S bands (Mackie, 1989). Usually RNA is considered intact when the intensity of the 23S rRNA bands seems to be twice that of the 16S rRNA band. In all the five lanes, the bands were sharp, clear and intense without smearing or background fluorescence in the lanes. The intensity of the 23S bands seemed to be twice that of the 16S bands. Starting from the left side of the gel, the first lane (lane 1) contained RNA extracted from wild type HG163. This RNA sample was not treated with RNase-free DNAse enzyme. In this lane (1), bacterial DNA could be seen present as a high molecular weight band near the well. Lane 2-5 contained RNA samples that were treated with RNAse free DNAse enzyme. In all these lanes, no bacterial DNA was present, thus demonstrating that the DNA was being removed from

the samples by the RNase-free DNAse enzyme. For mutants HG208, HG209 and HG210, RNA samples were also loaded on acrylamide gel and the results obtained were similar to the denaturating agarose gel shown above.

3.4.2 RNA quantity (concentration)

Concentration of RNA was calculated using the OD value read at 260nm (A_{260} reading, see Materials and Methods). RNA (1μg) of mutants and wild type were each treated with RNase-free DNAase enzyme to digest any contaminating bacterial DNA. The range of concentrations RNA extracted ranged from 200 to 3000 μg/ml. As expected, higher amounts of RNA were extracted from wild type, HG163 compared to the *atpG* mutants, due to higher cell densities. However, the amount of RNA was normalized so that the same amount of RNA was treated with RNase-free DNAse enzyme and reverse transcriptase.

3.4.3 Levels of pckA mRNA expression in atpG mutants and in wild type HG163

The levels of *pckA* mRNA expression in wild type HG163 and *atpG* mutants were determined by real time, reverse transcriptase PCR. From RNA extracted, cDNA was synthesised and used quantitatively to measure expression of *pckA* mRNA as described in Material and Methods (Section 2.4.3). Typical raw data (Fig. 15) and standard curve (Fig. 16) are shown, using *pckA*$^+$ plasmid, pHG51. The plasmid was linearized by digesting it with Xho I restriction enzyme. The concentrations of linearized plasmid DNA used for the standard curves were 30400, 3040, 304 and 30.40 pmol.

These standards were used in triplicate for every experiment and a plot of C_t value against fluorescence was generated for each standard as shown below in Fig. 15.

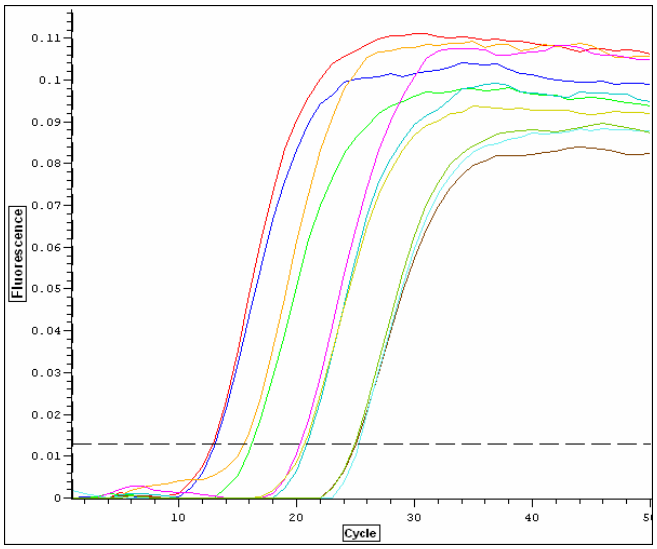

Fig. 15: Typical standard data for real-time RT-PCR. Curves show fluorescence versus time.

The standard curves generated by DNA Engine Opticon® 2 Real-time PCR Detection system in these runs produced linear results as shown by the graph generated in Fig. 16. The lowest R^2 value for the line of best fit for any experiment was 0.996. Graph produced was $C_{(t)}$ values against log concentration of *pckA* mRNA. In addition, we used known amounts of positive controls that were run alongside samples to determine the accuracy of the measurements. The anti-logs of concentrations of samples were then calculated and used to plot concentration of *pckA* mRNA versus time using Graph Prism 4.0.

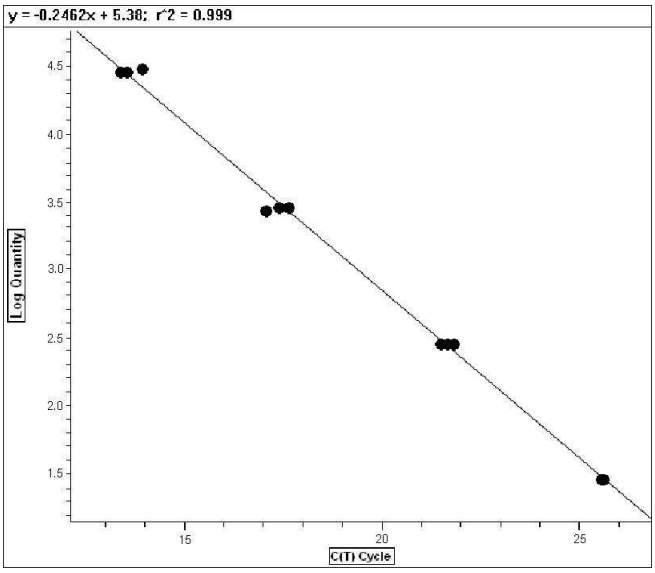

Fig. 16: A typical standard curve generated by DNA Engine Opticon® 2 Real-time PCR Detection system (by MJ research/Biorad research). Graph represents log of concentration (ranging from 30.4 pmol to 30.40 nmol) versus C_t cycle values against of pHG51.

The *pckA* mRNA levels were assessed in wild type HG163 and mutants (HG203, HG205 and HG206) (Fig. 17). The results showed that expression of *pckA* mRNA in the wild type HG163 started as early as 3 hours after inoculation, increased substantially at 5 hours, and peaked at 7 hours (Fig. 17). This time corresponded to early stationary as shown in Fig. 9. However, by 9 hours *pckA* mRNA expression in HG163 started to decrease. This decrease in *pckA* mRNA expression could be due to cessation of synthesis and RNA dilution as cells grow slowly in early stationary phase.

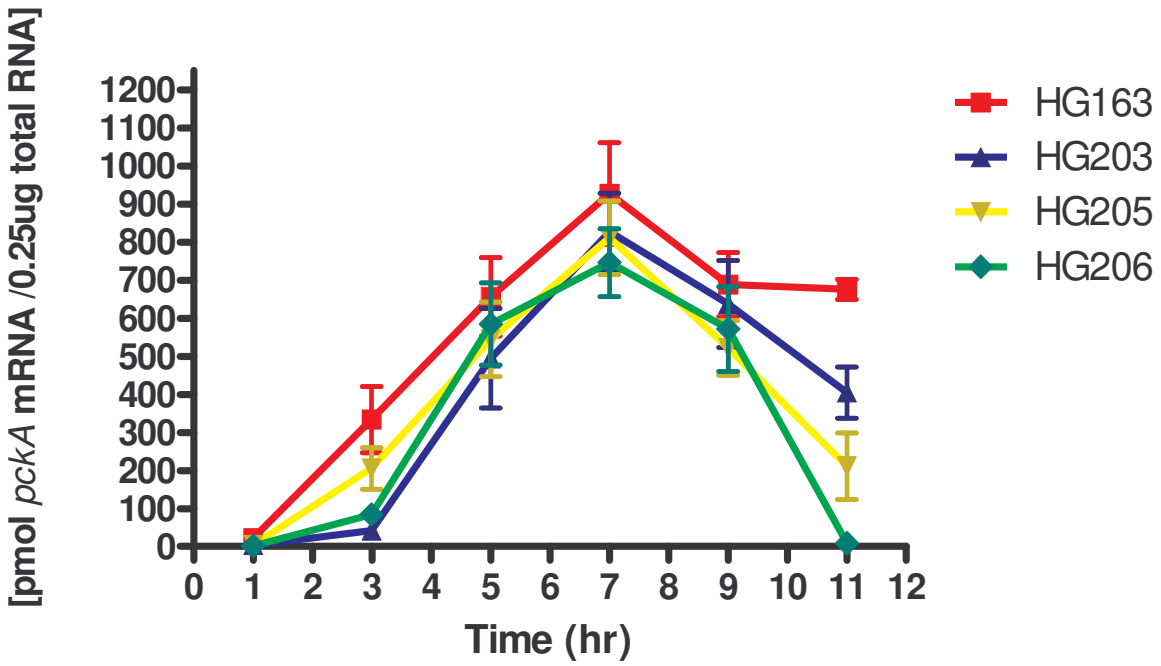

Fig. 17: *pckA* mRNA levels (pmol *pckA* mRNA/0.25ug total RNA) of wild type HG163, and *atpG* mutants (HG203, HG205, HG206). Error bars represent standard errors of the mean.

In the *atpG* mutants (HG203, HG205 and HG206), *pckA* mRNA expression starts at a lower rate at 3 hours but subsequently the level of expression is not significantly different from wild type (Fig. 17). By 9 hours, the expression of *pckA* mRNA decreased in all three *atpG* mutants. The highest expression of *pckA* mRNA occurred at 7 hours in HG203, HG205 and HG206. Growth was continued up to 11 hours in wild type and *atpG* mutants to see the expression of *pckA* mRNA expression in mid-stationary phase. It was observed that by 11 hours, in the *atpG* mutants, *pckA* mRNA expression decreased more sharply than in the wild type (Fig. 17).

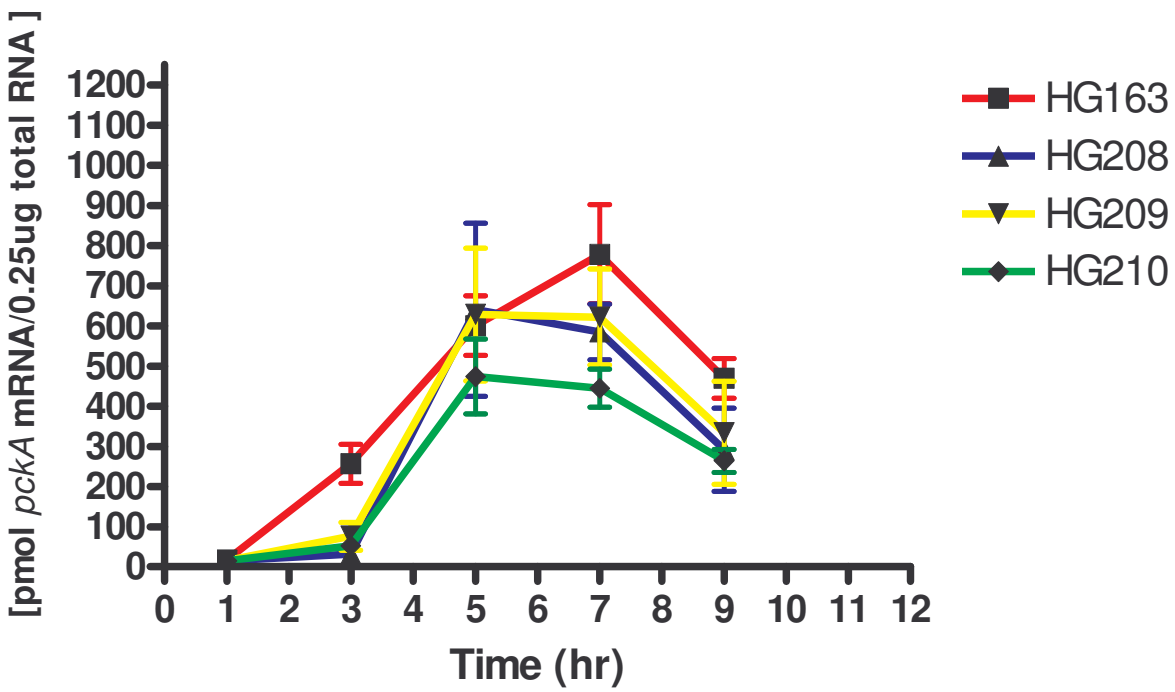

Fig. 18: *pckA* mRNA expression (pmol *pckA* mRNA/0.25ug total RNA) of wild type HG163, and *atpG* mutants (HG208, HG209 and HG210). Error bars represent standard errors of the mean.

Similarly, *pckA* mRNA expression was assessed in Gro^+ suppressors of *atpG* mutants (HG208, HG209, HG210) and in wild type HG163 (Fig. 18). The wild type strain HG163 demonstrated similar *pckA* mRNA expression pattern as previously shown. In the *atpG* mutants (HG208, HG209 and HG210), *pckA* mRNA started slowly at 3 hours and peaked at 5 to 7 hours. Subsequently the expression of *pckA* mRNA decreased somewhat (Fig. 18). The expression pattern was not significantly different from that found for HG203, HG205 and HG206.

These results suggest that there is no major difference in *pckA* mRNA expression between Gro^-, *atpG* mutants, Gro^+ suppressor mutants and wild type. This leads us to believe that the regulation of *pckA* by *atpG* or by its metabolic activity is not transcriptionally controlled but probably post-transcriptionally regulated.

3.5 Fluorescence quenching of Acridine orange as a measure of hydrogen ion flux in *atpG* isolates.

It has been shown that *atpG* mutants have defects in ATP-dependent proton pumping (Shin *et at.,* 1992). Since this defect could be responsible for the Pck^- phenotype by some mechanism, ATP dependent proton pumping was determined in the *atpG* isolates of Madhavan (2002).

Plasmid pDJK35 ($atpG^+$, Table 1) was shown to complement the Atp^-, Suc^-, kan^R, Gro^- and Pck^- phenotypes of the *atpG* isolates, HG203, HG205 and HG206 (Madhavan, 2002). ATP-dependent proton pumping was also determined for wild type, HG163 and for strains HG203, HG205 and HG206 with plasmid pDJK35 and with the plasmid vector, pACYC184, as controls.

3.5.1 Complementation of bacterial strains with vector plasmid and $atpG^+$ plasmid

Calcium-dependent transformation was unsuccessful for the *atpG* mutants (Madhavan, 2002 and this work). Therefore, pDJK35 and pACYC184 (Table 1) were electroporated into the *atpG* mutants and into wild type. The vector plasmid expresses tetracycline and chloramphenicol drug resistance while pDJK35 expresses only chloramphenicol drug resistance. Relevant phenotypes are shown in Table 4.

Table 4: Growth of bacterial strains on selective antibiotics plates.

Bacterial strains	LB plates containing chloramphenicol	LB plates containing tetracycline
HG163	-	-
HG203	-	-
HG205	-	-
HG206	-	-
HG163/pACYC184	NT	+
HG203/ pACYC184	NT	+
HG205/ pACYC184	NT	+
HG206/ pACYC184	NT	+
HG163/pDJK35	+	-
HG203/ pDJK35	+	-
HG205/ pDJK35	+	-
HG206/ pDJK35	+	-

NT: stands for not tested.

3.5.2 H^+ flux in inside-out vesicles.

Inside-out vesicles were prepared as discussed in section *2.3.1*. Volumes of membranes corresponding to 300 μg of protein (Lowry method, section *2.3.1*) were used to measure hydrogen ion flux as described in materials and methods (Section *2.6.2*).

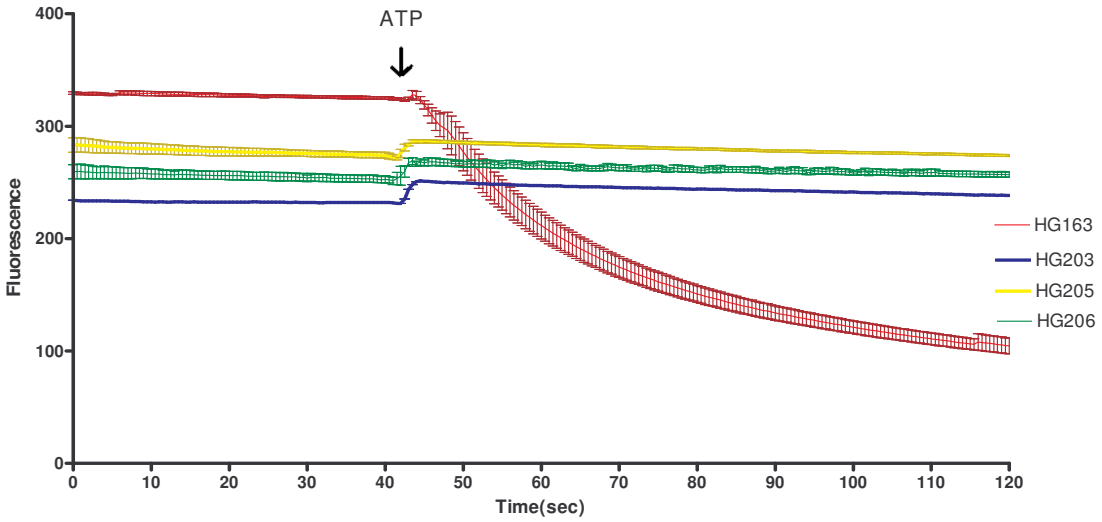

Fig. 19: Fluorescence quenching of acridine orange versus time in wild type HG163, HG203, HG205 and HG206. ATP (0.25 M) was added after 41 seconds. Error bars represent standard errors of the means.

The results of the fluorescence quenching acridine orange in wild type HG163 and *atpG* mutants (HG203, HG205 and HG206) are depicted in Fig. 19. As expected, in wild type, ATP synthase in the membrane was functional and thus when ATP was added there was a decrease in fluorescence due to pumping of hydrogen ions inside the membrane vesicles that caused protonation of acridine orange. In the *atpG* mutants, when ATP was added, there was no quenching of acridine orange. The small increase in fluorescence when ATP was added at 41 seconds in *atpG* mutants and in wild type, could be due to the intrinsic fluorescence of ATP.

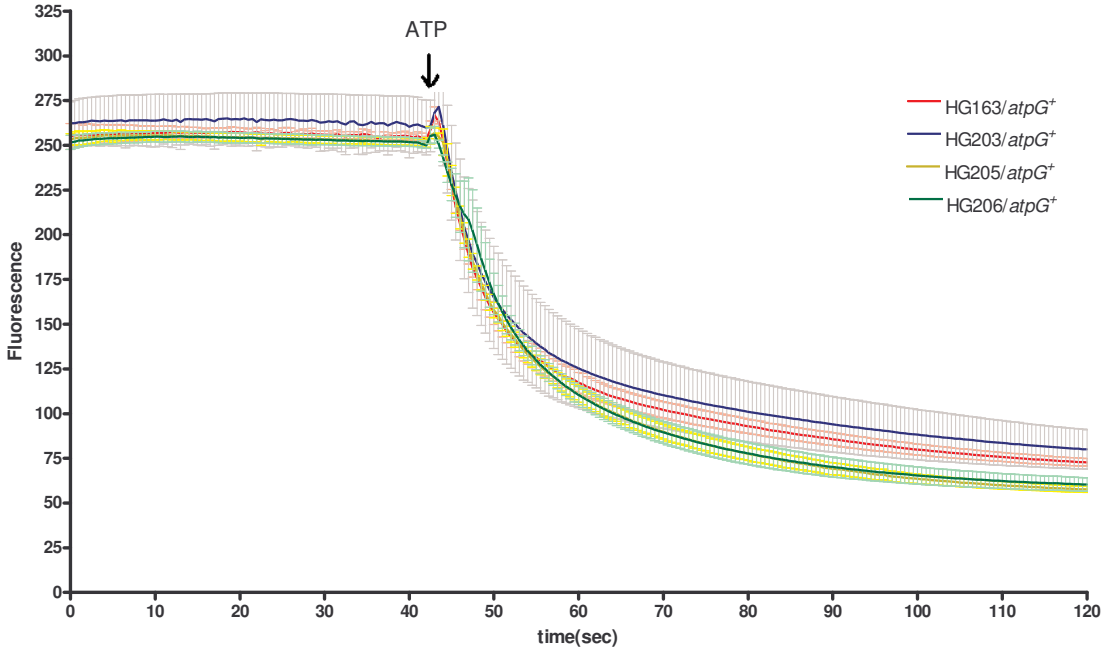

Fig. 20: Fluorescence quenching of acridine orange in wild type HG163 and *atpG* mutants (HG203, HG205 and HG206) complemented with *atpG*$^+$ plasmid. ATP (0.25M) was added at 41 seconds. Error bars represent standard errors of the means.

Figure 20 shows fluorescence quenching of acridine orange in inside out vesicles of wild type HG163 and *atpG* mutants (HG203, HG205 and HG206) that were complemented with *atpG*$^+$ plasmids. The presence of *atpG*$^+$ gene restored the functionality of ATP synthase in the mutants.

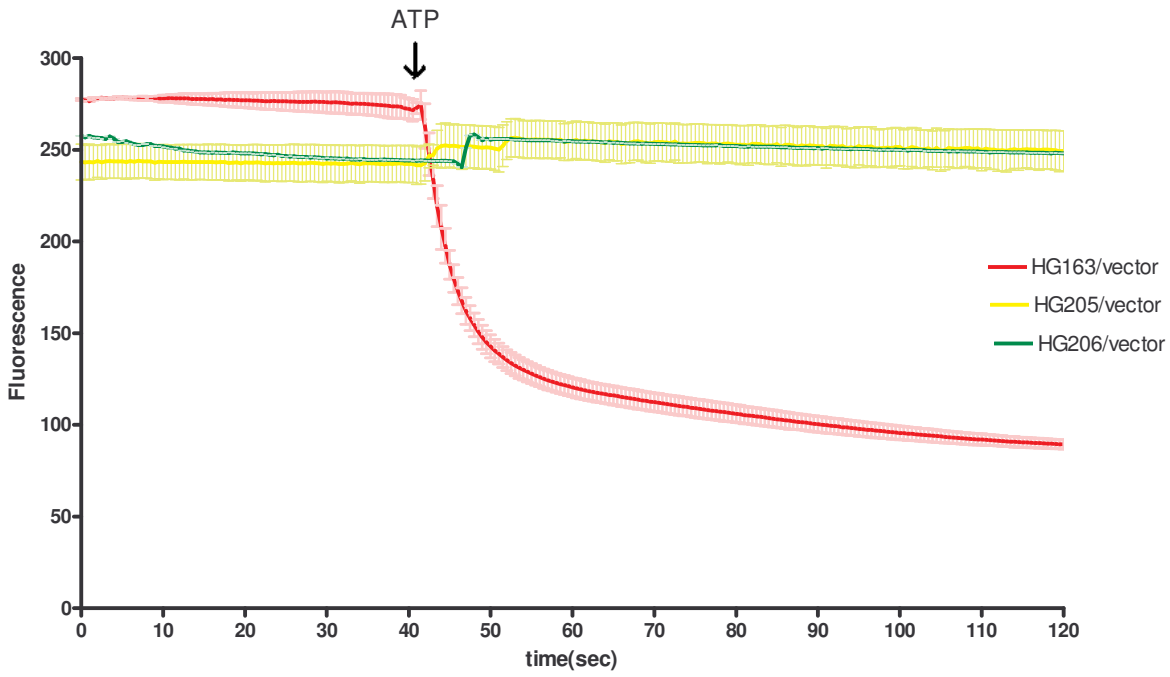

Fig. 21: Fluorescence quenching of acridine orange versus time in wild type and *atpG* mutants (HG205 and HG206) containing vector plasmid pACYC184. ATP (0.25M) was added at 41 seconds. Error bars represent standard errors of the means.

As expected, addition of plasmid vector pACYC184 did not alter the fluorescence profile in *atpG* mutants or wild type HG163. At 41 sec, when ATP was added there was decreased in fluorescence for HG163/ pACYC184 while for the *atpG* mutants with this vector, no change in fluorescence was observed.

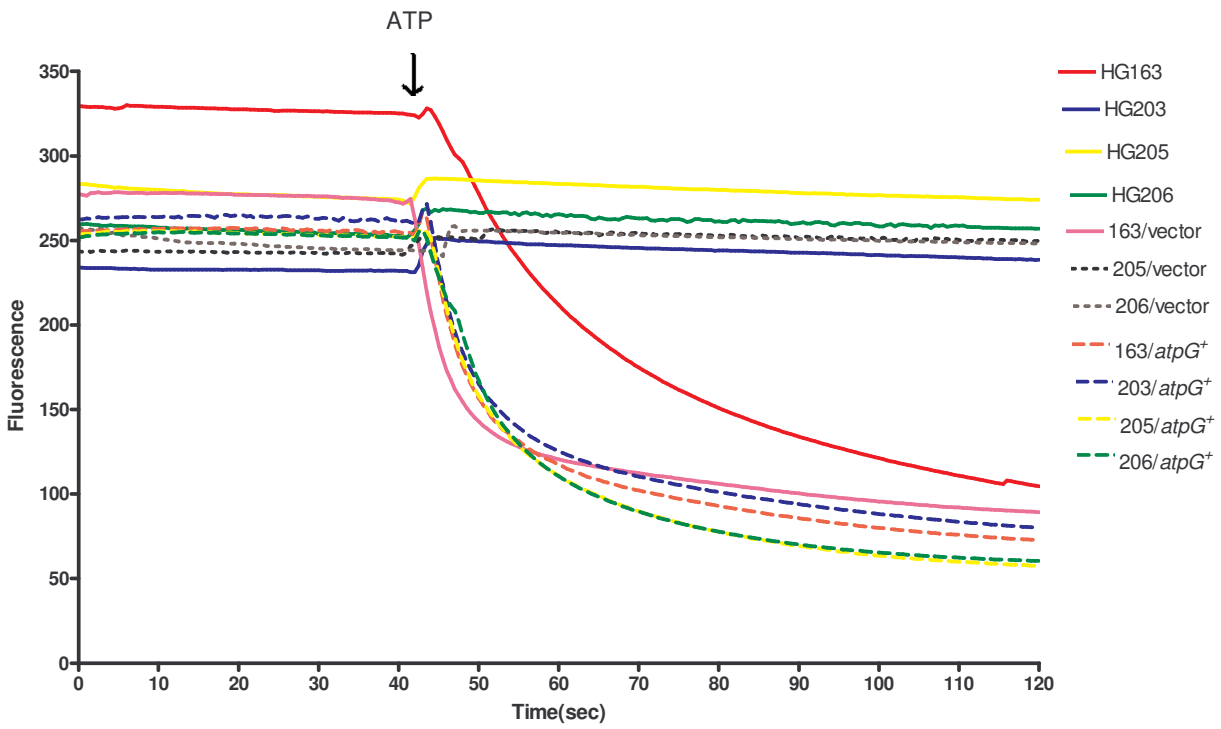

Fig. 22: A summary of all the graphs generated in the acridine orange experiment without the error bars.

A summary of all the experiments is shown in Fig. 22. This graph shows the change in fluorescence quenching in the *atpG* mutants as well as *atpG*$^+$ complemented mutants. It also indicates that the plasmid vector did not affect florescence quenching.

CHAPTER FOUR

4.0: Discussion and Conclusions

4.1 Phenotypes and growth of *atpG* mutants

4.1.1 Phenotype of atpG mutants

Previously, spontaneous *Suc*$^-$ *Pck*$^-$ mutants were isolated from strain HG163 (*pps*$^-$ *pckA*$^+$) (Madhavan, 2002). They were found to have pleotropic phenotypes (Gro$^-$, Atp$^-$ and kan^R) typical of *atp* mutants. The mutants were complemented by plasmids containing the *atpG* gene. The complete *atp* operons were sequenced in the mutants and they were found to have frame-shift mutations in the region encoding the C-terminus of the γ-subunit of the F_1F_0 Atp synthase (Madhavan, 2002).

When these *atpG* mutants were transduced to *pps*$^+$ using W3350 as a donor (Adhya *et al.,* 1968), they remained Suc$^-$ thus, the Suc$^-$ phenotypes are independent of *pps* and therefore not due to defects in the *pckA* gene. Boogerd *et al.,* (1998) also found that mutations in *atp* genes are Suc$^-$ and suggested that this could be due to uncoupling and disruption of the electrochemical gradient and/or to transport defects. Thorbjarnadothir *et al.,* (1978) found that mutations in *atp* genes could confer resistance to aminoglycoside drugs such as kanamycin. ATP mutants are probably resistant to kanamycin due to an altered electrochemical gradient, thus causing defects in the transport of aminoglycoside drugs into the cell. Hunbert and Altendorf, (1989), also showed that *atpG* mutations in the gamma (γ) subunit of ATP synthase conferred aminoglycoside resistance. Therefore, the phenotypes of the *atpG* mutants (HG203, HG205, HG206) were similar to what has been described for *atpG* mutants by others.

4.1.2 Growth yield and doubling time of atpG mutants.

Wild type HG163 grew at a faster rate and with a higher yield than *atpG* mutants (Fig.9, 10; Table 3). Downie *et al.,* (1980) have found that *atp* mutants have lower growth yields and Jensen *et al.,* (1993) also showed that *atp* mutants have lower growth rates and growth yields. This is because growth yield as described by Jensen *et al.,* (1993) is related to the coupling between growth and catabolism. Their data suggested that *E. coli* makes use of its ability to respire even if it cannot directly couple respiration to ATP synthesis, and in doing so, *E. coli* increases substrate level ATP synthesis. Thus, we observed the same reduced growth rates and yields for *atpG* mutants as others did.

HG203, HG205, HG206 had lower growth yields and growth rates (Gro^- phenotypes). However, Gro^+ suppressors were isolated from these strains (HG208, HG209 and HG210 respectively) which had higher growth yields (Table 3). Growth rates were not significantly affected in Gro^+ suppressors (Table 3).

4.2 Possible reasons for lower expression of *pckA* in *atpG* mutants.

Pck enzyme activity in *atpG* mutants, HG203, HG205 and HG206 were significantly lower (15-21% of wild type, HG163 Pck specific activity). These results confirmed that *atpG* mutations in *E. coli* have an effect on Pck specific activity as observed by Madhavan, 2002. Hypotheses were formulated as follows: (i) *atpG* mutations can alter *pckA* expression at the transcription level; (ii) *atpG* mutations alter translation, assembly or stability of PEP carboxykinase. These changes could be due to reduced ATP synthesis, to reduced proton gradient or due to changes in intra-cellular pH. Moreover, Gro^+ suppressors (HG208, HG209 and HG210) had Pck specific activities of 51% to 73% of wild type, HG163. The growth yields as shown above and

the increase in Pck specific activity suggested that HG208, HG209 and HG210 are partially reverted to Pck^+. The reason why this is happening is still unknown. However, Boogerd *et al.,* (1998) found that *E.coli atp* deletion strain LM2800, which cannot grow on minimal medium supplemented wih succinate as the only carbon source, was able to grow on succinate when left one week on succinate containing minimum media when incubated at 37^{o}C. This change from Suc^- to Suc^+ strain was due to a gene inactivation as determined by Boogerd *et al.,* (1998). They found that in these *atp* Suc^+ revertants, there is probably inactivation of *yhiF* gene. Usually in an *atp* mutant, ATP/ADP ratio is low, leading to decrease levels of negative supercoiling of DNA (Jensen and Michelson, 1995). Expression of the *yhiF* gene is enhanced by low levels of negative DNA supercoiling in *atp* mutants. The gene product of *yhiF* represses expression of the C_4-dicarboxylate transporter (*dstA*) gene, thus possibly preventing *atp* mutants from growing on 4-carbon sources such as succinate due to the transport defect.

The ability of other *atp* mutants to revert partially could explain why some of our mutants (HG208, HG209 and HG210) had growth yields and Pck specific activities partially reverted to wild type, although phenotypically, these mutants were still Suc^-, unlike the revertants reported by Boogert *et al.* (1998).

4.3 ATP synthase activities in *atpG* mutants.

In *atpG* mutants (HG203, HG205 and HG206), it was confirmed that ATP synthase specific activities were around 3.4% of wild type HG163. Gro^+ suppressors (HG208, HG209, HG210) also had low ATP synthase specific activites. This suggests that somehow the *pckA* activity was affected indirectly by *atpG*.

Increased glucose metabolism has been demonstrated in *atp* mutants (Jensen and Michelsen, 1992). They also found that during growth on minimal medium containing glucose, there was an increased flow of carbon through the glycolytic pathway and in the TCA cycle in these mutants.

Using transcriptome analysis, Noda *et al.,* (2006) did a DNA array analysis to compare gene expression in *atp* mutants compared to wild type strain. They found out that the expression of genes like *gltA* (citrate synthase), *icdA* (isocitrate dehydrogenase) , *sucA* (2-oxoglutalate dehydrogenase E1 component), *sucB* (dihydrolipoamide succinyltransferase component E2), *sucD (*succinyl-CoA synthetase α chain), *aceA* (isocitrate lyase), *aceB* (malate synthase A) and *mdh* (malate dehydrogenase) coding for enzymes in the TCA cycle were decreased to about 50% of wild type levels. Genes encoding the pyruvate dehydrogenase complex were upregulated two fold in *atp* mutants. Some genes involved in the synthesis of respiratory chain enzyme were also upregulated (such as *ndh,* encoding NADH dehydrogenase II, which increased 3.7 fold and *cydA*, cytochrome *d* oxidase subunit I, which increased two fold). Genes encoding flagellar formation and cellular structures (*ompF*) were repressed. Other genes that were repressed were *hupA* and *hupB* (encoding the DNA binding protein Hu), and *topA* (encoding DNA topoisomerase I). These studies suggested that *atp* mutations have multifactorial effects in *E.coli* and that *pckA* may be one of many genes that is affected indirectly.

4.4 Expression of *pckA* mRNA in *atpG* mutants

Goldie *et al.,* (1984) showed that at the onset of stationary phase in cells grown on LB, there was 100 fold induction of β-galactosidase activity in *pckA-lacZ* fusion

strains. In addition, they concluded that besides cAMP, there was another, unknown regulatory signal which is either required to inhibit *pckA* expression during log phase or to induce *pckA* expression during stationary phase.

The lower expression of Pck enzyme activity in the *atpG* mutants could be due to several factors. One of these factors included the possibility of *atpG* mutants affecting transcription of *pckA*: perhaps removing a regulatory signal that is required to induce *pckA* transcription during stationary phase. Mutations in the γ-subunit might have a regulatory effect on *pckA* at transcriptional, translational or post translational levels. In this study, we determined the level of *pckA* mRNA expression in the *atpG* mutants using real time RT- PCR.

During the growth curve of the *atpG* mutants and of wild type HG163, *pckA* mRNA levels were measured. The results indicated that the level of wild type, HG163, *pckA* mRNA had increase significantly by 3 hours and reached a maximum at the onset of stationary phase (7hrs). By 9 hrs, the level of *pckA* mRNA started to decrease, perhaps due to sessation of *pckA* transcription, accompanied by slow growth at this point.

From 1 hr to the onset of stationary phase, there was approximately 50-fold induction in *pckA* mRNA expression in wild type HG163. This fold in induction is about half of that observed by Goldie *et al.,* (1984). However, this work was done using *pckA-lacZ* fusions to measure β-galactosidase activities. There are several reasons why the fold induction of mRNA does not correlate with that of the fold induction in protein. Firstly, one molecule of *pckA* mRNA is not equivalent to one molecule of protein synthesised. Secondly, there are numerous RNA degradation pathways within *E. coli*

(Grunberg-Manago, 1999; Rauhut and Klug, 1999; Regnier and Arraiano, 2000) which are important regulatory mechanisms and *pckA-lacZ* mRNA could be more stable than *pckA* mRNA. Using subgenic-resolution oligonucleotide microarrays to study global RNA degradation in wild type *E. coli* MG1655, Selinger *et al.,* (2003) found that the half-life of total mRNA was 6.8 min. This suggested that degradation of mRNA is a fast and active process, thus the number of *pckA* mRNA molecules is a steady state value reflecting synthesis and degradation rates. Thirdly, Mohanty and Kushner (2006) found that the majority of *Escherichia coli* mRNAs undergo some form of transcriptional modification in exponentially growing cells. This is mainly caused by poly(A) polymerase, (PAP1). Deletion of the structural gene of PAP1 (*pinB*) caused a 90% reduction in poly(A) levels along with increased mRNA half-lives, while overproduction of PAP1 caused a reduction in mRNA stability and invariability (Mahanty and Kushner, 1999). These data suggest that there are numerous factors affecting mRNA stability and that they may be important in determining steady state levels of *pckA* mRNA.

The *atpG* mutants (HG203, HG205 and HG206) had similar patterns of *pckA* expression as wild type, with induction of mRNA starting at 3 hrs, peaking at 7 hrs and decreasing from 9 hrs onwards. These results suggest that *atpG* does not regulate *pckA* at the transcriptional level. Wild type levels appeared to be slightly higher throughout, but these differences were not statistically significant. The Gro^+ isolates, partially reverted in Pck enzyme levels and in growth yields, had similar mRNA profiles as wild type HG163. This confirms that *atpG* does not regulate *pckA* at the transcriptional level. This down regulation of expression of *pckA* by mutation in *atpG* is probably related to other factors such as translation, assembly or stability of Pck protein.

4.5 Proton flux in *atpG* mutants and wild type HG163

In inside-out vesicles, normally functioning ATP synthase will pump protons inside the vesicle. Acridine orange penetrates the membrane vesicles and emits fluorescence at 530 nm with an excitation of 490 nm. It combines with H^+ and is protonated (Rudnick, 1986). This leads to further difusion of acridine orange into the vesicles and quenching of fluorescence. Thus a normally functional ATP synthase inside-out vesicle, will pump protons inside the vesicle, leading to a decrease of fluorescence (Fig. 23).

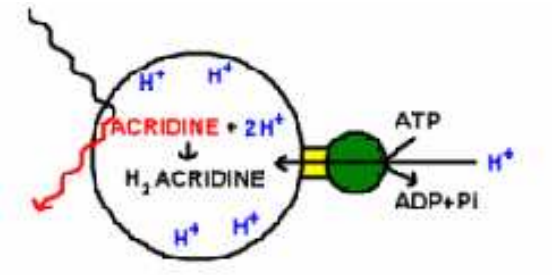

Fig. 23: Diagramatic representation of fluorescence quenching in inside-out vesicles. ATP synthase pumps protons inside the vesicle. Free acridine orange molecule emits fluorescence. However, when protonated, no fluorescence is emitted.

As expected, the ability of inside-out vesicles from wild type cells to pump H^+ in the presence of ATP, was demonstrated, whereas vesicles from the *atpG* mutants could not pump H^+ ions under these conditions. The mutants were complemented with an *atpG*$^+$ plasmid, and fluorescence quenching of acridine orange was completely restored. These results indicate that in the *atpG* mutants, there is no pumping of H^+ outside the cell by ATP synthase. Therefore the question that arises is whether in the *atpG* mutants there are disturbances in pH levels and if so, could the changes in pH influence the Pck expression. Usually in *E. coli* cells during aerobic growth, there is excretion of

membrane permeable weak acids that lead to an increase in intracellular pH. These weak acids concentrate down the pH gradient, thus acidifying the cytoplasm (Bock and Sawers, 1996). *E. coli* maintains its internal pH between 7.4 and 7.8 during aerobic growth (Lambert *et al.,* 1997). Thus we hypothesized that intracellular pH changes may affect expression of *pckA*.

In *Agrobacterium strain C58*, Liu *et al.,* (2005) showed that the *pckA* gene expression is dependent on the intracellular pH: with low pH, *pckA* will be induced. The *pckA* is located adjacent to the loci *chvG* and *chvI* genes that encode a two-component regulatory system important for virulence. These genes also control acid-inducible genes. Mantis and Winans, (1993) showed that the *chvI* gene of *Agrobacterium tumefaciens* complements an *E. coli phoB* mutation (*phoB* encodes alkaline phosphatase in *E. coli*). Bacteria use the *phoB-phoR* sensor/kinase system to sense external acidity (Suziedeliene *et al.,* 1999); although the *pho* regulon in *E. coli* is usually induced by phosphate starvation.

Goldie (unpublished results) has shown that growth of *E. coli* on LB medium without glucose (conditions leading to maximum expression of *pckA*) causes the medium to become alkaline, likely due to transport of amino acids into the cells. The increasing alkalinity of the medium could be accompanied by acidification of the cytoplasm. This would likely not occur in *atpG* mutants due to the permeability of their membranes to protons.

4.6 Conclusion

In this study, while working with *atpG* mutants, Gro^+ variants of the *atpG* mutants were isolated which were partially reverted in their Pck specific activities. These Gro^+ suppressor mutants have Pck activity 51% to 73% of wild type Pck activity. Growth curves and doubling time results also indicate that these Gro^+ suppressor mutants have higher growth yields even if their doubling time is not significantly different from the original *atpG* mutants. However, the ATP synthase activity of mutants and Gro^+ suppressor mutants is unchanged. It is very low compare to wild type indicating that these mutants and Gro^+ suppressor mutants are still Atp^-.

The *pckA* mRNA expression of the mutants and wild type was determined by real time RT-PCR to assess whether *atpG* mutations had effects on *pckA* transcription. Real time RT-PCR results indicate that there is no major difference in *pckA* mRNA expression in wild type, mutants and suppressor mutants. Thus, mutations in *atpG* do not have an effect on transcription of *pckA*.

Moreover, the H^+ ion flux was tested in the mutants and wild type by quenching of acridine orange fluorescence. These experiments demonstrate the inability of the *atpG* mutants to pump proton ions actively across the membrane. Thus these results suggest that the F_0 ATPase remaining in the *atpG* mutants could be only acting as a H^+ pore leading to an equilibrium state for H^+ inside and outside the cell. Changes in ΔH^+ or in pH inside or outside the cell membrane may affect the Pck induction and/or Pck activity.

Considering the original hypothesis: "**Mutations in *atpG* alter *pckA* transcription in *Escherichia coli*",** I can conclude that mutations in *atpG* do not affect

pckA transcription. Altered expression of Pck could be due to changes in translation, assembly or stability of the enzyme. Down regulation of *pckA* by mutations in *atpG* could also be related to other factors such as post transcriptional regulation, changes in ΔH^+ or changes in internal pH. It is also clear, however, that transcription of *pckA* increases about 50 fold in stationary phase by some other mechanism, since this was still observed in *atpG* mutants.

4.7 Future work

Since gluconeogenesis is an energy consuming process, the decrease in ATP production by ATP synthase in *atpG* mutants could be a factor in the decrease in Pck activity. If these mutants have pleotrophic effects on other gluconeogenic enzymes or Krebs cycle enzymes, especially if changes in intracellular pH, concentration of ATP or pH gradient are involved, then measuring the activity of these enzymes in the *atpG* mutants in log phase and stationary phase could be important. These activities were assayed and found to be normal by Deng Mapiour, a summer student; however, it was determined that this work was done with the strains which reverted to Gro^+ $Pck^{\pm}$ and it will have to be repeated.

The acridine orange experiment demonstrates that there is no flux of H^+ ions in the *atpG* mutants. Could the lack of a pH gradient be the cause of a lower level of Pck activity? This could be determined by first measuring the pH inside and outside the cells. Usually during respiration, H^+ ions are extruded and the pH outside the cell is more acidic. At the end of respiration, H^+ is passively transported inside the cell, thus causing an equilibrium inside and outside the cell (Kashket, 1985). The internal or intracellular pH can be calculated using a derivative of green fluorescence protein (GFP) designated

as ratiometric GFP (Olsen *et al*., 2002). The ratiometric GFP was obtained by introducing specific amino acid substitutions to the chromophore, causing the resulting protein to alter its excitation spectrum according to pH of the surrounding environment (Miesenböck *et al*., 1998). The *atpG* mutants could be transformed with a ratiometric GFP plasmid. Olsen *et al*., (2002) reported that they found excitation at 410 nm gave a strong pH dependent fluorescent signal and at 430 nm, a pH independent point was observed. The excitation ratio, fluorescence intensity at 410 nm and 430 nm ($R_{410/430}$) was found to be suitable as a measure of intracellular pH (pH_i). A calibration curve could be constructed that will correlate $R_{410/430}$ to pH_i. Cells could be grown at 37^{o}C in LB broth and then transformed with ratiometric GFP plasmid. The cells in buffers of different pH's could then be permeabilised with carbonyl cyanide-3-chlorophenylhydrazone (CCCP), which will disrupt the proton gradient, to generate a standard curve. Subsequently overnight cultures expressing ratiometric GFP could be harvested by centrifugation, washed twice in potassium phosphate buffer (pH 7.5) containing glucose (10 mM), and finally resuspended in potassium phosphate buffer (10 mM) with appropriate pH for 30 min. The bacterial suspension (10^8 cells) will then be applied to a coverslip coated with 0.01% poly-L-lysine and allowed to settle. Unattached bacteria will be removed by rinsing with buffer. Fluorescence will then be read with a fluorescence microscope. The initial range of the calibration curve could lie between pH 4.5 to 8.5. The $R_{410/430}$ will then be used to correlate to the calibration curve constructed with wild type to obtain the internal pH of wild type, *atpG* and *atpG* mutants complemented with *atpG* plasmid.

Appendix 1

RNA extraction method from Dr. G. A. Mackie (1989): Micro procedure

Grow your cultures to the desired density in LB; add rifampicin (freshly prepared in methanol) as needed.

Remove 320 µl of culture (with a P1000 pipettor) and add to 160 µl of 3x extraction buffer (1.5% SDS, 300 mM Na-acetate, pH ~6.0, 30 mM EDTA) in a microcentrifuge tube in a heating block set to 100 degrees C. Boil for 60 sec. Chill on ice.

Add 500 µl water-saturated phenol (pH 4.3; Fisher Scientific) and vortex well. Centrifuge at room temperature for 2 min at full speed in an microfuge.

Transfer the aqueous phase to 500 µl of phenol-chloroform-isoamyl alcohol (25:24:1). Leave the last 50-100 µl behind and avoid taking anything from the interface. Vortex well and spin as before. Transfer the aqueous phase to a fresh tube containing 500 µl of secondary butanol (2-butanol). Vortex well and spin for 15 sec.

The butanol is the upper phase - remove it and keep the lower aqueous phase. This step removes residual phenol and other non-polar compounds. At this stage you should have about 400-450 µl. If the volume of the aqueous phase is larger than this, you can repeat the 2-butanol extraction, but note that it will shrink the aqueous phase to about half its volume. You may have to add sterile water to get back to 400 µl volume.

Add about 30 µl of 3 M Na-acetate and 1 ml of 95% ethanol. Let precipitate overnight at -20 ^{o}C.

Recover by centrifugation at full speed for 10-15 min in the cold. You should obtain a somewhat translucent white pellet 1-2 mm in diameter. Drain thoroughly (use a pipettor) and let residual ethanol evaporate at room temperature for 15 minutes.

Dissolve the pellet in a sterile buffer containing 10 mM Tricine, pH 7.5, 100 mM Na-acetate, 1 mM EDTA and 800 mM ammonium acetate. Vortex briefly. Reprecipitate with 500 ul ethanol at -20 ^{o}C (overnight).

Recover the RNA by centrifugation (10-15 min at full speed). Drain well. Cover the pellet with 500 ul 80% ethanol, let sit on ice a few minutes, then spin again.

Let the final pellet air dry for >10 min (we never use a speed vac), then dissolve in 50 ul sterile water. Estimate the yield by the A260 using a 1:200 dilution. Expect to recover 35-50 µg of RNA in total.

Check RNA by separating 5 µg on an agarose (or polyacrylamide gel). The intensity of the 23S rRNA should be double that of the 16S - if not, there's been significant degradation.

Appendix 2

Quantitative PCR cycle:

Action	Temp(oC)	Time	Ramp time	Acquisition
1. UDG reaction	50	2 min	2°C / sec	no
2. UDG inactivation/ template denaturation	95	2 min	2°C / sec	no
3. Denaturation	95	15 sec	2°C / sec	no
4. Hybridisation	60	30 sec	2°C / sec	no
5. Elongation	72	30 sec	2°C / sec	no
6. Plate reading	-	-	0.2°C / sec	1 sec + plate read
7. Repeat steps 3 to 6 for 49 times	-	-	-	no
8. Incubation	95	1 sec	2°C / sec	no
9. Melting curve	60-95	1 sec hold	-	Read every 0.2°C
10. Incubation	25	30 min	-	-

Note:

A UDG incubation step before PCR cycling destroys any contaminating dU-containing product from previous reactions. UDG is then inactivated by the high temperatures during normal PCR cycling, allowing the amplification of genuine target sequences. (Invitrogen).

Appendix 3

Membrane isolation by the French Press method (Madhavan, 2002)

Cells were inoculated overnight in 300 ml of minimal media containing glucose and casamino acid. The next day, cells were centrifuged at 5000 rpm for 15 min at 4 ^{0}C. The pellets were resuspended in 50 mM Tris, (pH 7.8 + 5mM $MgSo_4$) and centrifuged at 5000 rpm for 15 min at 4^{0}C. Pellets were then washed twice with 200 ml 0.8% saline solution before spinning again at 5000 rpm for 15 min at 4^{0}C. Pellets were again resuspended in ice cold Tris-Mg EDTA buffer containing 1mM EDTA (1g/10 ml) before proceeding to French press at 1000 psi and centrifuge 12,000 rpm for 15 min at 4^{0}C. The supernatants collected were centrifuged at 17,640 X *g*/ 1hr at 4^{0}C in a 60 Ti rotor in a Beckman ultracentrifuge.

The pellets obtained were resuspended in 2 ml ice cold Tris-Mg EDTA buffer, homogenised with a hand held homogeniser and frozen at -70 ^{0}C for further use.

References

Adhya S., Cleary P., Campbell A. (1968). A deletion analysis of prophage lambda and adjacent genetic regions. *Proc.Natl. Acad. of Sci. USA. 61(3):956-962.*

Ames G. and Joshi A. (1990). Energy coupling in bacterial periplasmic permease. J. Bacteriol. 172: 4133-4137.

Bachman K., Ptashne M., Gilbert W. (1976). Construction of plasmids carrying the cI gene of bacteriophage lambda. Proc. Natl. Acad. Sci. USA. 73: 4174-4178.

Barth M., Marschall C., Muffler A., Fischer D. and Hengge-Aronis R. (1995). Role for the histone-like protein H-NS in growth phase-dependent and osmotic regulation of sigma S and many sigma S-dependent genes in *Escherichia coli*. J. bacteriol. 177: 3455-3464.

Becker G. and Hengge-Aronis R. (2001). What makes an *Escherichia coli* promoter sigma(S) dependent? Role of the -13/-14 nucleotide promoter positions and region 2.5 of sigma(S)**.** Mol. Microbiol. 39: 1153-1165.

Bertani I., Sevo M., Kojic M., and Venturi V. (2003). Role of GacA, LasI, RhlI, Ppk, PsrA, Vfr and ClpXP in the regulation of the stationary-phase sigma factor rpoS/RpoS in *Pseudomonas*. Archives of Microbiology. 180(4): 264-271.

Bock A. and Sawers G. (1996). Fermentation, p. 262-282. In Neidhardt F.C., Curtiss R. III, Ingraham J., Lin E., Low K., Magasanik B., Reznikoff W., Schaechter M. and Umbarger H. (ed.) *Escherichia coli* and *Salmonella*: Cellular and Molecular Biology, 2nd ed., Vol. 1. American Society of Microbiology, Washington, D.C.

Boogerd FC., Boe L., Michelsen O. and Jensen PR. (1998). *atp* mutants of *Escherichia coli* fail to grow on succinate due to a transport deficiency. J. Bacteriol. 180: 5855-5859.

Brosnan JT. (1999). Comments on metabolic needs for glucose and the role of gluconeogenesis. Eur. J. Clin. Nutri. 53, suppl. 1: 107-111.

Brown L. and Elliot T. (1996). Efficient translation of the RpoS sigma factor in *Salmonella typhinurium* requires host factor I, an RNA-binding protein encoded by the *hfq* gene. J. Bacteriol. 179: 656-662.

Brown L., Gentry D., Elliott T. and Cashel M. (2002). DksA affects ppGpp induction of RpoS at a translational level. J. Bacteriol. 184: 4455-4465.

Busby S. and Ebright RH**.** (2000). Transcription activation by catabolite activator protein (CAP). J. Mol. Biol. 293(2): 199-213.

Bustin SA. (2004). A-Z of quantitative PCR. International University Line, La Jolla, Ca.

Bustin SA., Benes V., Nolan T., Pfaffl MW. (2005). Quantitative real-time RT-PCR--a perspective. J. Mol. Endocrinol. 34: 597-601.

Capaldi RA. and Schulenberg B. (2000). The ε subunit of bacterial and chloroplast F_1F_0 ATPases. Structure, arrangement and role of the ε subunit in energy coupling within the complex. Biochim. Biophys. Acta. 1458: 263-269.

Capaldi RA., Schulenberg B., Murray J. and Aggeler R. (2000). Cross-linking and electron microscopy studies of the structure and functioning of the *Escherichia coli* ATP synthase. J. Exp. Biol. 203: 29-33.

Capaldi RA. and Aggeler R. (2002). Mechanism of the $F_{(1)}F_{(0)}$-type ATP synthase, a biological rotary motor. Trends Biochem. Sci. 27: 154-160.

Chan YH. (1987). Genetic fusions in loci affecting the synthesis of phosphoenolpyruvate carboxykinase in *Escherichia coli* K12. Msc thesis. University of Saskatchewan, Saskatoon, SK, Canada.

Chang AC. And Cohen SN. (1978). Construction and characterization of amplifiable multicopy DNA cloning vehicles derived from p15A cryptic mini plasmid. J. Bacteriol. 134: 1141-1156.

Chao YP., Patnaik R., Roof WD., Young RF. and Liao JC. (1993). Control of gluconeogenic growth by *pps* and *pck* in *Escherichia coli*. J. Bacteriol. 175: 6939-6944.

Colland F., Fujita N., Ishihama A. and Kolb A. (2002). The interaction between sigmaS, the stationary phase sigma factor, and the core enzyme of *Escherichia coli* RNA polymerase. Genes Cells. 7: 233-247.

Colland F., Fujita N., Kotlarz D., Bown JA., Meares CF., Ishihama A. and Kolb A. (1999). Positioning of sigma(S), the stationary phase sigma factor, in *Escherichia coli* RNA polymerase-promoter open complexes. EMBO J. 18: 4049-4059.

Cooper RA. And Kornberg HL. (1967). The direct synthesis of phosphoenolpyruvate from pyruvate in *Escherichia coli*. Proc. Royal Soc. London Ser. B. 168: 263-280.

de Crombruggh B., Busby S. and Buc H. (1984). Cyclic AMP receptor protein: role in transcription activation. Science. 224: 831-838.

Dheda K. Huggett JF. Chang JS. Kim LU. Bustin SA. Johnson MA. Rook GA. Zumla A. (2005). The implications of using an inappropriate reference gene for real-time reverse transcription PCR data normalization. Analytical Biochemistry. 344(1):141-3.

Diez M., Zimmermann B., Borsch M., Konig M., Schweinberger E., Steigmiller S., Reuter R., Felekyan S., Kudryavtsev V., Seidel CA. and Graber P. (2004). Proton-powered subunit rotation in single membrane-bound F_0F_1-ATP synthase. Nat. Struct. Mol. Biol. 11(2):135-41.

Dimroth P. (1990). Mechanisms of sodium transport in Bacteria. Phil. Trans. R. Soc. Lond. 326: 465-477.

Dimroth P., von Ballmoos C., Meier T., and Kaim G.(2003). Electrical power fuels rotary ATP synthase. Structure. 11(12):1469-73.

Dmitriev OY., Jones PC. and Fillingame RH. (1999). Structure of the subunit c oligomer in the F_1F_0 ATP synthase: model derived from solution structure of the monomer and cross-linking in the native enzyme. Proc. Natl. Acad. Sci. USA. 96: 7785-7790.

Dove SL. and Hochschild A. (2001). Bacterial two-hybrid analysis of interactions between region 4 of the sigma(70) subunit of RNA polymerase and the transcriptional regulators Rsd from *Escherichia coli* and AlgQ from Pseudomonas aeruginosa. J. Bacteriol. 183: 6413-6421.

Dove SL., Huang FW. and Hochschild A. (2000). Mechanism for a transcriptional activator that works at the isomerization step. Proc. Natl. Acad. Sci. USA. 97: 13215-13220.

Downie JA., Langman L., Cox GB., Yanofsky C. and Gibson F. (1980). Subunits of the Adenosine Triphosphatase complex translated *in vitro* from the *Escherichia coli unc* operon. J. Bacteriol. 143: 8-17.

Espinosa-Urgel M., Chamizo C. and Tormo A. (1996). A consensus structure for sigma S-dependent promoters. Mol. Microbiol. 21: 657-659.

Fillingame RH., Jiang W. and Dmitriev OY. and Jones PC. (2000). Structural interpretations of F_0 rotary function in the Escherichia coli F_1F_0 ATP synthase. Biochim. Biophys. Acta. 1458: 387-403. J. Exp. Biol. 203: 9-17.

Fillingame RH ., Angevine CM. and Dmitriev OY**.** (2002). Coupling proton movements to c-ring rotation in $F_{(1)}F_{(o)}$ ATP synthase: aqueous access channels and helix rotations at the a-c interface. Biochim Biophys Acta. 1555(1-3):29-36.

Fiske CH. and Sunnarow Y. (1925). The colometric determination of phosphorus. J. Biol. Chem. 66: 375-400.

Fonyó A., Palmieri F. and Quagliariello E. (1976). Carrier-mediated transport of metabolites in mitochondria. Horiz Biochem Biophys. 1976; 2:60-105.

Gaal T., Ross W., Estrem ST., Nguyen LH., Burgess RR. and Gourse RL. (2001). Promoter recognition and discrimination by EsigmaS RNA polymerase. Mol. Microbiol. 42: 939-954.

Gay NJ. and Walker JE. (1981). The *atp* operon: nucleotide sequence of the promoter and the genes for the membrane proteins and the δ subunit of the *Escherichia coli* ATP-synthase. Nucleic Acids Res. 9: 3919-3625.

Geiger PG. and Bessman SP. (1972). Protein determination by Lowry's method in the presence of sulfhydryl reagents. Anal. Biochem. 49: 467-473.

Gentry DR., Hernandez VJ., Nguyen LH., Jensen DB. and Cashel M. (1993). Synthesis of the stationary phase sigma factor σ^S is positively regulated by ppGpp. J. Bacteriol. 175: 7982-7989.

Girvin ME., Rastogi VK. Abildgaard F., Markley JL. and Fillingame RH.(1998). Solution structure of the transmembrane H^+-transporting subunit c of the F_1F_0 ATP synthase. Biochemistry. 37(25):8817-24.

Goldie AH. and Sanwal BD. (1980a). Genetic and physiological characterisation of *Escherichia coli* mutants defective in phosphoenolpyruvate carboxykinase activity.J. Bacteriol. 141: 1115-1121.

Goldie AH. and Sanwal BD. (1980b). Allosteric control by calcium and mechanism of desensitisation of phosphoenolpyruvate carboxykinase of *Escherichia coli*. J. Biol. Chem. 255: 1399-1405.

Goldie, H. (1984). Regulation of transcription of the *Escherichia coli* phosphoenolpyruvate carboxykinase locus: studies with *pck-lacZ* operon fusions. J. Bacteriol. 159: 832-836.

Grunberg-Manago M. (1999). Messenger RNA stability and its role in control of gene expression in bacteria and phages. Annu. Rev. Genet. 33: 193-227.

Hausrath AC., Gruber G., Mattews BW. and Capaldi RA. (1999). Structural features of the gamma subunit of the *Escherichia coli* $F_{(1)}$ ATPase revealed by a 4.4-A resolution map obtained by x-ray crystallography. Proc. Natl. Acad. Sci. USA. 96: 13697-13702.

Hazard AL. and Senior AE. (1994). Mutagenesis of subunit delta from *Escherichia coli* F_1F_0-ATP synthase. J.Biol. Chem. 269: 427-432.

Hermolin J. Dmitriev OY., Zhang Y. and Fillingame RH. (1999). Defining the domain of binding of F_1 subunit epsilon with the polar loop of F_0 subunit c in the *Escherichia coli* ATP synthase. J. Biol. Chem. 274: 15598-15604.

Hengge-Aronis R. (2002). Stationary phase gene regulation: what makes an *Escherichia coli* promoter sigmaS-selective?. Curr. Opin. Microbiol. 5: 591-595.

Hengge-Aronis R. (2002b). Signal transduction and regulatory mechanisms involved in control of the sigma(S) (RpoS) subunit of RNA polymerase. Microbiol. Mol. Biol. Rev. 66: 373-395.

Hirsch M. and Elliott T. (2002). Role of ppGpp in rpoS stationary-phase regulation in *Escherichia coli*. J. Bacteriol. 184: 5077-5087.

Hunbert R. and Altendorf K. (1989). Defective γ subunit of ATP synthase (F_1F_0) from *Escherichia coli* leads to resistance to aminoglycoside antibiotics. J. Bacteriol. 171: 1435-1444.

Ishihama A. (2000). Functional modulation of Escherichia coli RNA polymerase. Annu. Rev. Microbiol. 54: 499-518.

Jahreis K. Lengeler JW. (1993). Molecular analysis of two ScrR repressors and of a ScrR-FruR hybrid repressor for sucrose and D-fructose specific regulons from enteric bacteria. Molecular Microbiology. 9(1):195-209.

Jensen PR and Michelsen D. (1992). Carbon and energy metabolism of *atp* mutants of *Escherichia coli*. J. bacteriol. 174: 7635-7641.

Jensen PR., Westerhoff HV and Michelson O. (1993). The use of *lac*-type promoters in control analysis. EMBO 12(4): 1277-1282.

Jensen PR., Michelsen D. and Westerhoff HV. (1995). Experimental determination of control by the H(+)-ATPase in *Escherichia coli*. J. Bioenerg. Biomembr. 27(6): 543-554.

Jiang W. and Fillingame RH. (1998). Interacting helical faces of subunits a and c in the F_1F_0 ATP synthase of *Escherichia coli* defined by disulfide cross-linking. Proc. Natl. Acad. Sci. USA. 95: 6607-6612.

Jishage M. and Ishihama A. (1995). Regulation of RNA polymerase sigma subunit synthesis in *Escherichia coli*: intracellular levels of sigma 70 and sigma 38. J. Bacteriol. 177: 6832-6835.

Jishage M. and Ishihama A. (1998). A stationary phase protein on *Escherichia coli* with binding activity to the major σ subunit of RNA polymerase. Proc. Natl. Acad. Sci. USA. 95: 4953-4958.

Jishage M and Ishihama A. (1999). Transcriptional organization and in vivo role of the *Escherichia coli rsd* gene, encoding the regulator of RNA polymerase sigma D. J. Bacteriol. 181: 3768-3776.

Jishage M, Dasgupta D and Ishihama A. (2001). Mapping of the Rsd contact site on the sigma 70 subunit of *Escherichia coli* RNA polymerase. J. Bacteriol. 183: 2952-2956.

Jones HM., Brajkocvich CM. and Gunsalus RP. (1983). In vivo 5' terminus and lengh of the mRNA for the proton translocating ATPase (*unc*) operon of *Escherichia coli*. J. Bacteriol. 155: 1279-1287.

Kaback HR. (1990). Lac permease of *Escherichia coli* on the path of the proton. Phil. Trans., R. soc. Lond. B. 326: 425-436.

Kaim G, Mathey U and Dimroth P. (1998). Mode of interaction of the single a subunit with the multimeric c subunits during the translocation of the coupling ions by F_1F_0 ATPases. EMBO J. 17: 688-695.

Kashket ER. (1985). The Proton Motive Force in bacteria: A critical assessment of methods. Annu. Rev. Microbiol. 39: 219-242.

Kasimoglu E., Park S., Malek J., Tseng CP. and Gunsalus RP. (1996). Transcriptional regulation of the proton-translocating ATPase (*atp IBEFHAGDC*) operon of *Escherichia coli*: control by cell growth rate. J. Bacteriol. 178: 5563-5567.

Kleckner N., Bender J. and Gottesman S. (1991). Uses of transposons with emphasis on Tn*10*. Meth. Enzymol. 204: 139-180.

Klionsky DJ. and Simoni RD. (1985). Assembly of a functional F_1 of the proton translocating ATPase of *Escherichia coli*. J. Biol. Chem. 260: 11200-11206.

Kornberg A, Rao NN and Ault-Riche D. (1999). Inorganic polyphosphate: a molecule of many functions. Annu. Rev. Biochem. 68: 89-125.

Kotewicz ML., D'Alessio JM., Driftmier KM., Blodgett KP. and Gerard GF. (1985). Cloning and overexpression of Moloney murine leukemia virus reverse transcriptase in *Escherichia coli*. Gene. 35(3): 249-258.

Krulwich TA. (1990). Bacterial Energetics. The Bacteria, Vol. XII. Academic Press. San Diego, U.S.A.

Lambert LA., Abshire K., Blankenhorn D. and Zlonczewski JL. (1997). Proteins induced in *Escherichia coli* by benzoic acid. J. Bacteriol. 179: 7595-7599.

Lange R. and Hengge-Aronis R. (1994). The cellular concentration of the subunit of RNA polymerase in *Escherichia coli* is controlled at the levels of transcription, translation and protein stability. Genes Dev. 8: 1600-1612.

Lange R., Fischer D. and Hengge-Aronis R. (1995). Identification of transcriptional start sites and the role of ppGpp in the expression of rpoS, the structural gene for the σ^{38} subunit of RNA polymerase in *Escherichia coli*. J. Bacteriol. 177: 4676-4680.

Lee MH., Hebda CA. and Nowak T. (1981). The role of cations in avian liver phosphoenolpyruvate carboxykinase catalysis. Activation and regulation. J. Biol. Chem. 256: 12793-12801.

Lee SJ. and Gralla JD. (2001). Sigma 38 (rpoS) RNA polymerase promoter engagement via -10 region nucleotides. J. Biol. Chem. 276: 30064-30071.

Lengeler JW. (1993). Carbohydrate transport in bacteria under environmental conditions, a black box? Anton. Van. Leeuwenhoek. 63: 275-288.

Leslie AG. and Walker JE. (2000). Structural model of F_1-ATPase and the implications for rotary catalysis. Phil. Trans. R. Soc. Lond. B. 355: 465-472.

Liu P., Wood D. and Nester EW. (2005). Phosphoenolpyruvate carboxykinase is an acid-induced, chromosomally encoded virulence factor in *Agrobacterium tumefaciens*. J. Bacteriol. 187: 6039-6045.

Livak KJ. and Schmittgen TD. (2001). Analysis of relative gene expression data using real-time quantitative PCR and the 2(-Delta Delta $C_{(T)}$) Method. Methods. 25: 402-408.

Lowry OH., Rosebrough NJ., Farr AL. And Randall RJ. (1951). Protein measurement with the Folin phenol reagent. Journal of Biological Chemistry. 193(1):265-75.

Lynch AS. and Lin EC. **(**1996). Transcriptional control mediated by the ArcA two-component response regulator protein of *Escherichia coli*: characterization of DNA binding at target promoters. J. Bacteriol. 178(21):6238-49.

Madhavan S. (2002). Mutations in *atpG* encoding the gamma subunit of ATP synthase cause lowered expression of *pckA* in *Escherichia coli*. PhD Thesis, University of Saskatchewan, Saskatoon, SK, Canada.

Mackie GA. (1989). Stabilization of the 3' one-third of *Escherichia coli* ribosomal protein S20 mRNA in mutants lacking polynucleotide phosphorylase. J. Bacteriol. 171(8): 4112-4120.

Maeda H., Fujita N and Ishihama A. (2000). Competition among seven *Escherichia coli* sigma subunits: relative binding affinities to the core RNA polymerase. Nucl. Acids Res. 28: 3497-3503.

Mantis NJ. and Winans SC. (1993). The chromosomal response regulatory gene *chvI* of *Agrobacterium tumefaciens* complements an *Escherichia coli phoB* mutation and is required for virulence. Journal of Bacteriology. 175(20): 6626-36.

Matte A., Goldie H., Sweet RM. and Delbaere LTJ. (1996). Crystal structure of *Escherichia coli* phosphoenolpyruvate carboxykinase: a new structural family with the P-loop nucleoside triphosphate hydrolase fold. J. Mol. Biol. 256:126-143.

McLachlin DT., Coveny AM., Clark SM. and Dunn SD. (2000). Site-directed cross-linking of b to the alpha, beta, and a subunits of the *Escherichia coli* ATP synthase. J. Biol. Chem. 275: 17571-17577.

Meadow ND., Fox DK. and Roseman S. (1990). The bacterial phosphoenolpyruvate: glucose phosphotransferase system. Annu. Rev. Biochem. 59: 491-542.

Medina V, Pontarollo R., Glaeske D., Tabel H. and Goldie H. (1990). Sequence of the *pck* gene of *Escherichia coli* K-12: relevance to genetic and allosteric regulation and homology of *E. coli* phosphoenolpyruvate carboxykinase with the enzymes from *Tryponosoma brucie* and *Saccharomyces cerevisiae*. J. Bacteriol. 172: 7151-7156.

Miesenböck G., De Angelis DA. and Rothman JE. (1998). Visualizing secretion and synaptic transmission with pH-sensitive green fluorescent proteins. Nature. 394: 192-195.

Miller JH. (1972). Experiements in Molecular genetics. Cold Spring Harbor laboratories. Cold Spring Harbor. New York. U.S.A

Miller MJ., Oldenburg M. and Fillingame RH. (1990). The essential carboxyl group in subunit c of the F1F0 ATP synthase can be moved and H^+-translocating function retained. Proc. Natl. Acad. Sci. USA. 87(13):4900-4.

Mohanty BK. and Kushner SR. (1999). Analysis of the function of *Escherichia coli* poly(A) polymerase I in RNA metabolism. Mol. Microbiol. 34: 1094-1108.

Mohanty BK. and Kushner SR. (2006). The majority of *Escherichia coli* mRNAs undergo post-transcriptional modification in exponentially growing cells. Nucl. Acids Res. 34(19): 5695-5704.

Muffler A., Fischer D. and Hengge-Aronis R. (1996). The RNA binding protein HF-1, known as a host factor for phage Qβ RNA replication, is essential for *rpoS* translation in *Escherichia coli*. Genes Dev. 10: 1143-1151

Muffler A., Barth M., Marschall C. and Hengge-Aronis R. (1997a). Heat shock regulation of sigmaS turnover: a role for DnaK and relationship between stress responses mediated by sigmaS and sigma32 in *Escherichia coli*. J. Bacteriol. 179: 445-452.

Muffler A., Fischer D., Altuvia S., Storz G. and Hengge-Aronis R. (1996). The response regulator RssB controls stability of the sigma(S) subunit of RNA polymerase in *Escherichia coli*. EMBO J. 15: 1333-1339.

Mukhopadhyay S., Audia JP., Roy RN. and Schellhorn HE. (2000). Transcriptional induction of the conserved alternative sigma factor RpoS in *Escherichia coli* is dependent on BarA, a probable two-component regulator. Mol. Microbiol. 37: 371-381.

Murakami KS. and Darst SA. (2003). Bacterial RNA polymerases: the whole story. Curr. Opin. Struct. Biol. 13(1):31-39.

Nadanaciva S., Weber J. and Senior AE. (2000). New probes of the F_1-ATPase catalytic transition state reveal that two of the three catalytic sites can assume a transition state conformation simultaneously. Biochemistry. 39: 9583-9590.

Nakamoto RK., Ketchum CJ., Al-Shawi MK. (1999). Rotational coupling in the F_0F_1 ATP synthase. Annu. Rev. Biophys. Biomol. Struct. 28: 205-234.

Nakano T., Ikegami T., Suzuki T., Yoshida M., Akutsu H.(2006). A new solution structure of ATP synthase subunit c from *Thermophilic bacillus* PS3, suggesting a local conformational change for H^+-translocation.J Mol Biol. 21;358(1):132-44.

Negre D., Oudot C., Prost J., Murakami K., Ishihama A., Cozzone AJ., Cortay J. (1998). FruR-mediated transcriptional activation at the *ppsA* promoter of *Escherichia coli.* J. Mol. Biol. 276: 355-365.

Noda S., Takezawa Y., Mizutani T., Asakura T., Nishiumi E., Onoe K., Wada M., Tomita F., Matsushita K and Yokota A. (2006). Alterations of cellular physiology in *Escherichia coli* in response to oxidative phosphorylation impaired by defective F_1-ATPase. J. bacteriol. 188: 6869-6876.

Notley L. and Ferenci T. (1995). Differential expression of *mal* genes under cAMP and endogenous inducer control in nutrient-stressed *Escherichia coli*. Mol. Microbiol. 16(1): 121-129.

Ogilvie I., Aggeler R .and Capaldi RA. (1997). Cross-linking of the delta subunit to one of the three alpha subunits has no effect on functioning, as expected if delta is a part of the stator that links the F_1 and F_0 parts of the *Escherichia coli* ATP synthase. J. Biol. Chem. 272: 16652-16656.

Olivares-Zavaleta N., Jauregui R. and Merino E. (2006). Genome analysis of Escherichia coli promoter sequences evidences that DNA static curvature plays a more important role in gene transcription than has previously been anticipated. Genomics. 87(3):329-37.

Olsen KN., Budde BB., Siegumfeldt H., Rechinger KB., Jakobsen M. and Ingmer H. (2002). Noninvasive measurement of bacterial intracellular pH on a single-cell level with green fluorescent protein and fluorescence ratio imaging microscopy. Appl. Environ. Microbiol. 68(8): 4145-4147.

Oshima T., Aiba H., Masuda Y., Kanaya S., Sugiura M., Wanner BL. (2002). Transcriptome analysis of all two-component regulatory system mutants of *Escherichia coli K-12.* Mol. Microbiol. 46: 281-291.

Pernestig AK., Melefors O., and Georgellis D. (2001). Identification of UvrY as the cognate response regulator for the BarA sensor kinase in *Escherichia coli*. J. Biol. Chem. 27**6**: 225-231.

Phue JN., Noronha SB., Hattacharyya R., Wolfe AJ. and Shiloach J**.** (2005) Glucose metabolism at high density growth of *E. coli* B and *E. coli* K: differences in metabolic pathways are responsible for efficient glucose utilization in *E. coli* B as determined by microarrays and Northern blot analyses. Biotech. & Bioengin. 90(7): 805-20.

Plumbridge J. (2001). Regulation of PTS gene expression by the homologous transcriptional regulators, Mlc and NagC, in *Escherichia coli* (or how two similar repressors can behave differently). J. Mol. Microbiol. And Biotech. 3(3): 371-380.

Porter AC., Brusilow WS. and Simoni RD. (1983). Promoter for the *unc* operon of *Escherichia coli*. J. Bacteriol. 155: 1271-1278.

Pratt LA. and Silhavy TJ. (1996). The response regulator SprE controls the stability of RpoS. Proc. Natl. Acad. Sci. USA. 93: 2488-2492.

Ramseir TM., Bledig S., Michotey V., Feghali R., Saier MH. (1995). The global regulatory protein FruR modulates the direction of carbon flow in *Escherichia coli*. J. Molecular Microbiol. 16: 1157-1169.

Rastogi VK. and Girvin M. (1999). Structural changes linked to proton translocation by subunit c of the ATP synthase.Nature. 402: 263-268.

Rauhut R. and Klug G. (1999). mRNA degradation in bacteria. FEMS Microbiol. Rev. 23: 353-370.

Regnier P. and Arraiano CM. (2000). Degradation of mRNA in bacteria: emergence of ubiquitous features. Bioessays. 22: 235-244.

Rockabrand D., Livers K., Austin T., Kaiser R., Jensen D., Burgess R. and Blum P. (1998). Roles of DnaK and RpoS in starvation-induced thermotolerance of *Escherichia coli.* J. Bacteriol. 180: 846-854.

Romeo T., Gong M., Liu MY. And Brun-Zinkernagel AM. (1993). Identification and molecular characterisation of *csrA* a pleiotrophic gene from *Escherichia coli* that affects glycogen biosynthesis, gluconeogenesis, cell size and surface properties. J. Bacteriol. 175: 4744-4755.

Rudnick G. (1986). ATP-driven H+ pumping into Intracellular organelles. Ann. Rev. Physiol. 48:403-13.

Sabnis N., Yang H. and Romeo T. (1995). Pleiotropic regulation of central carbohydrate metabolism in *Escherichia coli* via the gene *csrA*. J. Biol. Chem.. 270: 29096-29104.

Saier Jr MH. and Chin AM. (1990). Energetics of bacterial phosphotransferase system in sugar transport and the regulation of carbon metabolism, p. 273-299. Krulwich, T.A. (ed. The bacteria. Vol XII. Acad. Press. Inc., San Diego, U.S.A.

Sanwal BD. (1970). Allosteric control of amphobolic pathways in bacteria. Bacteriol. Rev. 34: 20-39.

Schweder T., Lee HK., Lomovskaya O. and Matin A. (1996). Regulation of *Escherichia coli* starvation sigma factor (sigma s) by ClpXP protease. J. Bacteriol. 178: 470-476.

Schulenberg B., Wellmer F., Lill H., Junge W., Engelbrecht S. (1997). Cross-linking of chloroplast F_0F_1-ATPase subunit epsilon to gamma without effect on activity. Epsilon and gamma are parts of the rotor. Eur J. Biochem. 249: 134-141.

Selinger DW., Saxena RM., Cheung KJ., Church GM. and Rosenow C.(2003). Global RNA half-life analysis in *Escherichia coli* reveals positional patterns of transcript degradation. Genome Research. *13(2):216-23.*

Shiba T., Tsutsumi K., Yano H., Ihara Y., Kameda A., Tanaka K., Takahashi H., Munekata M., Rao NN. and Kornberg A. (1997). Inorganic polyphosphate and the induction of *rpoS* expression. Proc. Natl. Acad. Sci. USA. 94: 11210-11215.

Shin K., Nakamoto RK., Maeda M. and Futai M. (1992). F_0F_1-ATPase γ subunit mutations perturb the coupling between catalysis and transport. J.Biol. Chem. 267: 20835-20839.

Sledjeski DD., Gupta A .and Gottesman S. (1996). The small RNA, DsrA, is essential for the low temperature expression of RpoS during exponential growth in Escherichia coli. EMBO J. 15: 3993-4000.

Stock D., Leslie AG. and Walker JE. (1999). Molecular architecture of the rotary motor in ATP synthase. Science. 286: 1700-1705.

Sudom A., Walters R., Pastushok L., Goldie D., Prasad L., Delbaere LT. and Goldie H. (2003). Mechanisms of activation of phosphoenolpyruvate carboxykinase from *Escherichia coli* by Ca2+ and of desensitization by trypsin. J. Bacteriol. 185(14): 4233-4242.

Suziedeliene E., Suziedelis K., Garbenciute V. and Normark S. (1999). The acid-inducible *asr* gene in *Escherichia coli*: transcriptional control by the *phoBR* operon. J. Bacteriol. 181(7): 2084-2093.

Tanaka K., Handel K., Loewen PC., Takahashi H. (1997). Identification and analysis of the *rpoS*-dependent promoter of *katE*, encoding catalase HPII in *Escherichia coli*. Biochim. Biophys. Acta. 1352: 161-166.

Tari LW., Matte A., Goldie H. and Delbaere LT. (1997). Mg^{2+}-Mn^{2+} clusters in enzyme catalysed phosphoryl transfer reactions. Nature Structural Biology. 4(12): 990-4.

Thorbjarnadottir SH., Magnusdottir RA. and Eggertsson G. (1978). Mutations determining generalised resistance to aminoglycoside antibiotics in *Escherichia coli*. Mol. Gen. Genet. 161: 89-98.

Ueguchi C., Misonou N. and Mizuno T. (2001). Negative control of *rpoS* expression by phosphoenolpyruvate: carbohydrate phosphotransferase system in *Escherichia coli*. J. Bacteriol. 183: 520-527.

Utter MF. and Kurahashi K. (1954). Purification of oxaloacetic carboxylase from chicken liver. J. Biol. Chem. 207: 787-802

Venturi V. (2003). Control of *rpoS* transcription in *Escherichia coli* and *Pseudomonas*: why so different?. Mol. Microbiol. 49(1): 1-9.

Von-Meyenburg K., Jorgnsen BB., Nielsen J. and Hansen FG. (1982). Promoters of the *atp* operon coding for the membrane bound ATP synthase of *Escherichia coli* mapped by Tn*10* insertion mutations. Mol. Gen. Genet. 188: 240-248.

Walker JE., Saraste M. and Gay NJ. (1984). The *unc* operon. Nucleotide sequence, regulation and structure of ATP- synthase. Biochim. Biophys. Acta. 768:164-200.

Weber J. and Senior AE. (2000). ATP synthase: what we know about ATP hydrolysis and what we do not know about ATP synthesis. Biochim. Biophys. Acta. 1458: 300-309.

Weber J. and Senior AE. (2001). Bi-site catalysis in F1-ATPase: does it exist? J. Biol. Chem. 276: 35422-35428.

Weber J., Muharemagic A., Wilke-Mounts S., and Senior AE. (2004). Analysis of sequence determinants of F_1F_0-ATP synthase in the N-terminal region of alpha subunit for binding of delta subunit. J. Biol. Chem. 279(24): 25673-9.

Westblade LF., Ilag LL., Powell AK., Kolb A., Robinson CV. and Busby SJW. (2004). Studies of the *Escherichia coli* Rsd-sigma70 complex. J. Mol. Biol. 335: 685-692.

Wilkens S., Zhou J., Nakayama R., Dunn SD. and Capaldi RA. (2000). Localization of the delta subunit in the *Escherichia coli* $F_{(1)}F_{(0)}$-ATPsynthase by immuno electron microscopy: the delta subunit binds on top of the $F_{(1)}$. J. Mol. Biol. 295: 387-391.

Wright JA. and Sanwal BD. (1969). Regulatory mechanisms involving nicotinamide adenine nucleotides as allosteric effectors. II. Control of PEPCK. J. Biol. Chem. 244: 1838-1845.

www.ambion.com

www.invitrogen.com/content.cfm?pageid=3978#HowLuxWorks

www.qiagen.com/HB/plasmid purification

www.micro.biol.ethz.ch/op/ op_semdipl_dimroth2.htm

http://core.img.cas.cz/index.php?page=samples

Yamashino T., Ueguchi C. and Mizuno T. (1995). Quantitative control of the stationary phase-specific sigma factor, sigma S, in *Escherichia coli*: involvement of the nucleoid protein H-NS. EMBO J. 14: 594-602.

Zhang A., Altuvia S., Tiwari A., Argaman L., Hengge-Aronis R. and Storz G. (1998). The *oxyS* regulatory RNA represses *rpoS* translation by binding Hfq (HF-1) protein. EMBO J. 17: 6061-6068.

Zhou Y. **Gottesman** S. (1998). Regulation of proteolysis of the stationary-phase sigma factor RpoS. J. Bacteriology. 180(5):1154-8.

Zillig W, Palm R and Heil A. (1976). Cold Spring Harbor Laboratory, Cold Spring Harbor, New York.